HHS Public Access

Author manuscript

Biochim Biophys Acta. Author manuscript; available in PMC 2019 February 01.

Published in final edited form as:

Biochim Biophys Acta. 2018 February ; 1860(2): 586–599. doi:10.1016/j.bbamem.2017.11.014.

Non-bilayer Structures in Mitochondrial Membranes Regulate ATP Synthase Activity

Sardar E. Gasanov[*,§], **Aleksandr A. Kim**[*], **Lev S. Yaguzhinsky**[§], and **Ruben K. Dagda**[**]

[*]Applied Mathematics and Informatics Department, M.V. Lomonosov Moscow State University Branch, 22-a Amir Timur Avenue, Tashkent 100061, Uzbekistan

[§]Bioenergetics Department, A.N. Belozersky Institute of Physico-Chemical Biology, M.V. Lomonosov Moscow State University, Vorobievy Gory, Moscow 119991, Russia

[**]Department of Pharmacology, University of Nevada, Reno School of Medicine, 1664 North Virginia Street, Reno, Nevada 89557, USA

Abstract

Cardiolipin (CL) is an anionic phospholipid at the inner mitochondrial membrane (IMM) that facilitates the formation of transient non-bilayer (non-lamellar) structures to maintain mitochondrial integrity. CL modulates mitochondrial functions including ATP synthesis. However, the biophysical mechanisms by which CL generates non-lamellar structures and the extent to which these structures contribute to ATP synthesis remain unknown. We hypothesized that CL and ATP synthase facilitate the formation of non-bilayer structures at the IMM to stimulate ATP synthesis. By using ^{1}H-NMR and ^{31}P-NMR techniques, we observed that increasing the temperature (8 °C to 37 °C), lowering the pH (3.0), or incubating intact mitochondria with CTII - an IMM-targeted toxin that increases the formation of immobilized non-bilayer structures - elevated the formation of non-bilayer structures to stimulate ATP synthesis. The F_0 sector of the ATP synthase complex can facilitate the formation of non-bilayer structures as incubating model membranes enriched with IMM-specific phospholipids with exogenous DCCD-binding protein of the F_0 sector (DCCD-BPF) elevated the formation of immobilized non-bilayer structures to a similar manner as CTII. Native PAGE assays revealed that CL, but not other anionic phospholipids, specifically binds to DCCD-BPF to promote the formation of stable lipid-protein complexes. Mechanistically, molecular docking studies identified two lipid binding sites for CL in DCCD-BPF. We propose a new model of ATP synthase regulation in which CL mediates the formation of non-bilayer structures that serve to cluster protons and ATP synthase complexes as a mechanism to enhance proton translocation to the F_0 sector, and thereby increase ATP synthesis.

Graphical abstract

To whom correspondence should be addressed: Sardar E. Gasanov, Ph.D. sgasanov@yahoo.com; Ruben K. Dagda, Ph.D. rdagda@medicine.nevada.edu.

Conflicts of Interest

The authors do not have any conflict of interests to report for this study.

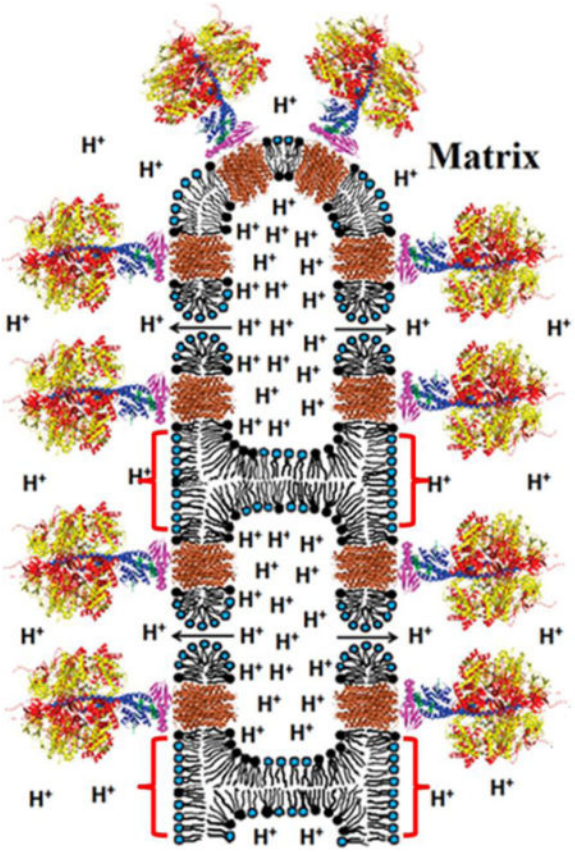

Keywords

Nonbilayer structures; Mitochondria; Cardiotoxin; ATP Synthase; Inverted Micelles; Cardiolipin

1.0 Introduction

The ATP synthase complex is a large multimeric enzyme complex comprised of over 20 subunits. More than half of the subunits that form the F_0 sector of the ATP synthase complex are submerged within the inner membrane of mitochondria (IMM) [1, 2]. The transport of H^+ through the F_0 sector of the ATP synthase complex is generated by establishing and mantaining a transmembrane proton gradient [1, 2]. ATP synthesis mediated by the ATP synthase complex is accomplished via the rotation of the central stalk and a ring of c-subunits (outer c subunits in bovine ATP synthase) in the membrane domain [3]. The active form of ATP synthase complex consist of a dimer that is maintained via a “dimerization interface” whereas the monomer form of ATP synthase is inactive [4, 5]. These dimers of ATP synthase have been localized at the apex of cristae, a site that serves as a proton trap to increase efficiency of ATP synthase [4]. Moreover, ATP synthase can undergo multiple conformations by forming large oligomers that consist of rows of dimers imbedded within cristae via an “oligomerization interface” to remodel cristae morphology. Interestingly, neither cristae morphology nor the energetic status of mitochondria govern dimerization or oligomerization of ATP synthase suggesting the existence of unidentified biophysical

mechanisms [6, 7] that maintain the active conformation of ATP synthase. Based on the recent high resolution X-ray crystal structural data, the F_0 sector of ATP synthase is comprised of c subunits (8 c subunits in bovine or 10 in yeast ATP synthase) radially arranged around the stalk structure [3, 8–10]. Importantly, the crystal structure of the F_0 c-ring has been solved by different research groups. For instance, in yeast, the high resolution crystal structure of the c-ring consists of 10 C subunits assembled in an hour-glass shaped structure that harbors a strong hydrophobic center. One of the subunits (subunit 9 in yeast) identified as dicyclohexylcarbodiimide (DCCD)-binding protein (DCCD-BPF) is involved in proton translocation through the F_0 c-ring of the ATP synthase [11]. The inner and outer rings of the N-terminal and C-terminal α-helices are mantained by hydrophobic interactions and make few interactions with water [12, 13]. Moreover, each C subunit of the F_0 consist of four α-helical fragments contains a strong hydrophobic core. The C subunit of F_0 is a hairpin containing two transmembrane-helices, connected by a short, partially ordered loop. The first two helices form the N-terminal transmembrane domain whereas the last two helixes from the C-terminal helix traverses the phospholipid membrane to anchor the protein to the IMM [12].

There is evidence that suggest the existence of non-bilayer structures - small lipid structures that exist in a non-lamellar phase - in specific regions of the IMM. These non-bilayer structures are required to maintain mitochondrial structural integrity and essential mitochondrial functions including regulating the calcium uniporter, transacylation reactions of phospholipids, and proton translocation to the F_0 sector of ATP synthase [14–17]. Importantly, non-bilayer structures have been shown to exist in organelles under physiological conditions to drive critical enzymatic reactions within specialized microdomains [16, 18].

Cardiolipin (CL), an anionic non-bilayer phospholipid, is required to maintain normal mitochondrial structure, promote mitochondrial fusion, and stimulate oxidative phosphorylation [19, 20]. In addition, CL can also act as a proton trap to shuttle protons to the ATP synthase complex to regulate ATP synthesis [2, 21]. Furthermore, CL, but not other anionic phospholipid, can mediate the formation of non-bilayer structures in mitochondria, presumably via its interaction with mitochondrial proteins [22]. Phosphatidylethanolamine (PE), a major neutral mitochondrial phospholipid, tends to form hexagonal phase structures, a particular form of non-bilayer structures. However, to date, it is not known if a structural polymorphism of PE is mediated via its interaction with mitochondrial proteins.

Although the structural organization of the ATP synthase complex and the molecular mechanisms by which the ATP synthase complex produces ATP have been well characterized [1], it is not known how non-bilayer structures, CL and the ATP synthase interplay to regulate mitochondrial functions (e.g. ATP synthesis).

Here, we hypothesized that CL interacts with the F_0 sector of ATP synthase to facilitate the formation of transient non-bilayer structures in the IMM as a mechanism to enhance ATP levels in mitochondria. Overall, by using a myriad of biophysical techniques, our data show that immobile non-bilayer structures in mitochondria govern ATP synthesis via the following biophysical mechanism. First, an elevation of the proton gradient leads to a lower pH at the

IMM space which destabilizes the bilayer packing of acidic phospholipids and induces lipid phase transitions (from a lamellar to a non-bilayer structure) within specific regions of the IMM that are in close proximity to the DCCD-BPF (C subunit) of the F_0 sector. Mechanistically, CL, but not other anionic phospholipids, binds to the F_0 sector of ATP synthase to facilitate the transition from a bilayer to non-bilayer phase of immobilized phospholipids in the IMM. This immobile non-bilayer structures, presumably an inverted micelle or similar structures, are organized in such a way that favors both the oligomerization of the F_0 sector and act as a specialized proton trap to shuttle protons to the ATP synthase complex leading to enhanced ATP synthesis.

2.0 Materials and Methods

2.1 Reagents

Egg yolk L-α-phosphatidylcholine (PC), cardiolipin (CL) from *E.coli*, bovine brain L-α-phosphatidyl-L-serine (PS), egg yolk L-α-phosphatidic acid (PA), and potassium ferricyanide were purchased from Sigma Chemical Co. (St. Louis, MO). All phospholipids were further purified on silica columns. Central Asian cobra *Naja naja oxiana* crude venom was obtained as a gift from Prof. L.Ya. Yukelson (Institute of Biochemistry, Uzbekistan Academy of Sciences) in lyophilized form. Cardiotoxins CTII and CTI, also known as cytotoxin CTII (or Vc5) and cytotoxin CTI (or Vc1) respectively, were isolated from 500 mg of crude venom as previously published [23] and were further purified by cation exchange HPLC by using a SCX 83-C-13-ET1 Hydropore column as previously described [24]. The purity of CTII and its molecular weight were assessed by Native-PAGE (Fig. 5C). The molecular weight of CTII is approximately 7 kDa. Based on the Native-PAGE assay, the purity of “gradient-purified” CTII is high (~99%) based on the absence of noticeable contaminating protein bands (Fig. 5C, lane B). All other reagents were from Sigma-Aldridge (Moscow, Russia).

2.2 Preparation of isolated mitochondria and exogenous DCCD-binding protein

Bovine heart mitochondria were isolated as previously described using sequential centrifugation steps [14, 25]. In brief, the final crude mitochondrial pellet was re-suspended in 5 ml of washing medium (0.3 M mannitol, 10 mM MOPS, 1 mM EDTA, and 0.1% (w/v) BSA at pH 7.4). The re-suspended mitochondria were osmotically shocked with 5 ml of 20% (w/v) sodium succinate in washing medium for 10 min. to release water soluble, phosphate-containing molecules of non-phospholipid nature. This step is necessary to simplify the ^{31}P-NMR spectra, thereby facilitating the analyses of the organization and molecular mobility of mitochondrial bilayers. The osmotically-shocked mitochondria were allowed to recover in an isotonic environment by immediately diluting the mitochondria in 40 ml of ice-cold washing medium (0.3 M mannitol, 10 mM MOPS, 1 mM EDTA, and 0.1% (w/v) BSA at pH 7.4), followed by centrifugation at 11,000 × *g* for 10 min. The supernatant was then decanted and the mitochondrial pellet was re-suspended in 5 ml of washing medium to a final concentration of 60 mg/ml which was sufficient for three independent ^{31}P-NMR experiments. Following an incubation of 20 minutes, 1.5 mM sodium succinate was added to 0.1 ml of re-suspended mitochondria as a substrate for oxidative phosphorylation, and quality control tests were performed in order to assess for the functional quality of

mitochondria. In brief, respiratory control index (RCI) ratios of mitochondria recovered in isotonic medium (0.3 M mannitol, 10 mM MOPS, 1 mM EDTA, and 0.1% (w/v) BSA at pH 7.4) after resuspension, were assayed in the presence of 1.5mM succinate as a substrate for complex II. By using a Clark electrode, RCI was then measured as the ratio of the O_2 consumption rate following the addition of 4 mM ADP and Pi divided by the O_2 consumption rate after all ADP has been converted to ATP. The RCI values for untreated mitochondria (baseline) were observed to be between 3–4, a range that is consistent with high quality, functional mitochondria [26]. Moreover, this result suggest that mitochondria are highly coupled (oxidative phosphorylation and ATP synthesis), even after subjecting mitochondria to osmotic shock as previously reported [22].

Mitochondrial samples (derived from the same stock: 1.5 ml of mitochondria in washing buffer with a protein concentration of 60 mg/ml and phospholipid concentration 6.3×10^{-2} M) were subjected to different treatments. For data shown in Figure 1, mitochondria were incubated at increasing temperatures within their NMR tubes while their ^{31}P-NMR signals were allowed to accumulate for 30 minutes (Fig. 1). To manipulate the amount of non-bilayer structures that are generated in mitochondria, mitochondria were treated with cardiotoxin II (9×10^{-4} M CTII), cardiotoxin I (9×10^{-4} M CTI), or with cobra venom phospholipase A_2 (PLA_2, 1×10^{-7} M PLA_2) at 15 °C in a control sample (Fig. 2). Immediately after NMR spectra were recorded, ATP content (amount of ATP residing in mitochondria, not the rate of ATP synthesis) in mitochondrial samples treated with CTII or CTI and/or PLA_2 and in untreated sample controls was measured using a protocol as previously described to assess mitochondrial content [27] with minor modifications. To stop further ATP synthesis, 0.5 ml of mitochondria taken from NMR tube were lysed by 20 minutes incubation in 5 ml of a buffer (0.8% Triton X-100, 1mM D-luciferin, 2.5 μg Photinus pyralis (firefly) luciferase per mg of mitochondrial proteins, 10 mM MOPS buffer, 5 mM MgSO4, 0.1 M ethylenediaminetetraacetic acid, and 1 mM dithiothreitol at pH 7.4). Following an incubation of 20 minutes at room temperature, the luminescence intensities were read using a luminometer (Berthold Technologies) at 22°C at several time intervals to obtain stable luminescence signals. The relative luciferase units were then converted to ATP concentrations by employing a curve of luminescence intensities based on known ATP concentrations (standards). To determine the extent that the reported ATP concentrations are specific for ATP synthase activity, an aliquot of the same mitochondrial samples from the same stock were treated with oligomycin (1μM), an irreversible inhibitor of the ATP synthase, prior to treatment with CTII, CTI, PLA_2 or with increasing temperature, which completely abolished ATP synthesis (data not shown).

In addition, consistent with our functional analyses of isolated mitochondria, we observed that the ^{31}P-NMR spectra of mitochondria recovered in isotonic solution (with or without a DANTE saturation, Fig. 1) is characteristic of mitochondria retaining normal structural integrity of the OMM and IMM and lack the presence of “contaminating” mitochondrial fragments and submitochondrial particles as previously described [22] (see Results 3.1 section). To calculate the absolute amount of phospholipids contained in each mitochondrial sample, the integral intensity of the ^{31}P-NMR signals from the experimental mitochondrial samples were normalized to the integral intensity of the ^{31}P-NMR signals obtained from multilamellar liposomes containing known phospholipid concentrations. Each ^{31}P-NMR

experimental condition was repeated at least three times with technical replicates for each mitochondrial sample. The phospholipid concentration for each mitochondrial fraction analyzed by ^{31}P-NMR was approximately 6.3×10^{-2} M. It is worth noting that each technical replicate for ^{31}P-NMR study yielded a variance of 8% between samples. The ATP synthase activity was expressed as μmol of ATP synthesized per mg of mitochondrial proteins as calculated from triplicate measurements from the ^{31}P-NMR sample tubes. To reduce technical variability in the assay, all mitochondrial samples derived from same stock of isolated bovine mitochondria. It is important to note that some level of ADP and P_i (not visually detected by ^{31}P-NMR) remained in mitochondria following osmotic shock and recovery in isotonic solution. Indeed, a significant level of mitochondrial content was measured in mitochondria following osmotic shock with succinate (see Figure 1, untreated mitochondria contained a significant amount of ATP at 37 and 40°C). It is worth noting that the sample per sample variation was observed to be less than 8% (± 4%) and the differences in results between experiments were less than 5%.

A fraction of proteolipids containing dicyclohexylcarbodiimide (DCCD)-binding protein was isolated from mitochondria as previously described [14]. In brief, the adenine nucleotide transport protein, and most of the remaining endogenous phospholipids, were removed by incubating the fraction with lysolecithin at 25 °C for 1 h. and subsequently purified by centrifugation on a sucrose density gradient as described [28]. Following gradient centrifugation, the pellet was extracted with 0.5% sodium deoxycholate and precipitated with $(NH_4)_2SO_4$ at 45% saturation. The precipitate was rinsed four times with mitochondrial wash buffer (20mM Tris-HCl buffer, pH 7.5, 0.5 mM dithiothreitol, 0.5 mM EDTA, and 1 mM $MgSO_4$) to remove any residual phospholipids and $(NH_4)_2SO_4$. The resulting product was termed “gradient-purified DCCD-BPF” and its molecular weight was determined by Native-PAGE (~8 kDa). Based on the Native-PAGE assays, the purity of “gradient-purified DCCD-BPF “is high (~99%) given the absence of noticeable contaminating protein bands (Fig. 5C, lane A). The binding of the purified product to dicyclohexylcarbodiimide (DCCD) was assayed according to Sebald et al. [29].

2.3 Preparation of multilamellar liposomes

Multilamellar liposomes were prepared by hydrating a dried lipid film. In brief, phospholipids in chloroform were dried via the continuous exposure of the sample to helium in vacuum for 1.5 h in order to form a lipid film. The film was then hydrated in a buffer containing 10 mM Tris-HCl, pH 7.4, 0.5 mM EDTA, and 0.1 M NaCl in 30% ^2H_2O and 70% ^1H_2O.

In addition, to study the effects of low pH on the formation of non-bilayer structures, some multilamellar samples were hydrated with a buffer at a pH of 3.0. The lipid suspension was then vortexed for 15 min. and the multilamellar liposomes were incubated in helium atmosphere for 4 h at 15 °C. The DCCD-BPF or cardiotoxin CTII were either added into multilamellar liposomes from an aqueous solution or were reconstituted into a lamellar phase by mixing a protein and phospholipids in a chloroform/methanol (1:1 by volume) solution. The organic solvent was then removed in vacuum and the protein-lipid films were hydrated as described above.

2.4 Preparation of unilamellar liposomes

Unilamellar liposomes were prepared by drying phospholipids in chloroform to form a lipid film as described above, but containing the following minor modifications. The hydration of a lipid film was performed in a ^2H_2O buffer containing 10 mM Tris-HCl, pH 7.4, and 0.5 mM EDTA. The lipid suspension was sonicated for 15 min in helium media at 4°C by employing an ultrasonic disperser USDN-1(St. Petersburg, Russia) at a frequency of 22 kHz. Unilamellar liposomes were then centrifuged at 200 × *g* for 60 min to remove heavy phospholipid aggregates, and incubated in helium atmosphere for 15 h at 10°C. The DCCD-BPF dissolved in methanol or cardiotoxin CTII in a ^2H_2O-containing buffer were added directly into unilamellar liposomes.

The phospholipid composition of unilamellar or multilamellar liposomes contained PC, PA, PS and CL at molar ratios of 6.5, 0.6, 0.4 and 2.5, respectively. In addition, the total concentration of phospholipids in unilamellar and multilamellar liposomes was approximately 1.4×10^{-2} M and 6.3×10^{-2} M respectively. The concentration of DCCD-BPF added in unilamellar or reconstituted in multilamellar liposomes was 2×10^{-4} M and 9×10^{-4} M respectively. The concentration of cardiotoxin CTII in multilamellar liposomes and in unilamellar liposomes were approximately 9×10^{-4} M or 2×10^{-4} M respectively. To determine the ability of CTII or DCCD-BPF to permeate unilamellar liposomes, 10 μl of saturated $K_3Fe(CN)_6$ solution in ^2H_2O buffer was added per 1 ml of liposomes.

To measure the stable association of CL, PA, PS or PC with either DCCD-BPF or CTII, phospholipids or proteins of interest were incubated in an assay buffer containing 30% ^2H_2O and 70% ^1H_2O, 10 mM Tris-HCl, pH 7.5, 0.5 mM EDTA and 1% Triton X-100. In brief, phospholipids or DCCD-BPF were added to the assay buffer dissolved in chloroform/methanol (1:1 by volume), whereas CTII dissolved in water (30% ^2H_2O and 70% ^1H_2O) was added to the assay buffer. The protein concentration in the assay buffer was 2×10^{-6} M whereas the concentration of phospholipids in the assay buffer was 8.4×10^{-6} M for PC and 4.8×10^{-6} M for acidic phospholipids (CL, PA or PS).

For testing the effects of various phospholipids (CL, PA, PS) on the oligomerizarion of DCCD-BPF or CTII, 4.8×10^{-6} M of protein and 7.2×10^{-5} M of phospholipids were incubated in a buffer containing 10 mM Tris-HCl, pH 7.5, 0.5 mM EDTA, 1% Triton X-100 for 1 hr at 15 °C. The weight of protein–phospholipid complexes was estimated by native PAGE as described in figure 5c.

The purity and quality of the multilamellar liposomes were observed to be high as the physical state of phospholipids in liposomes monitored by ^{31}P-NMR (multilamellar liposomes) and ^{1}H-NMR (sonicated unilamellar liposomes) was consistent with a liquid crystalline with a lamellar packing of phospholipids (Fig. 3–4).

2.5 ^{31}P-NMR and ^{1}H-NMR studies

^{31}P-NMR spectra of isolated mitochondrial fractions or multilamellar liposomes, and ^{1}H-NMR spectra of unilamellar liposomes, were recorded at 15 °C, unless indicated otherwise, by employing a Varian XL-200 spectrometer (USA) that was set with the following conditions. The ^{31}P-NMR spectra were recorded at an operating frequency of 80.99 MHz,

and proton broad-band decoupling was performed by continuous irradiation with the 90° pulse set at 12 μs, a power of 20 kHz, and a distance between pulses of 0.8 s. To improve the signal to noise ratio, the free induction decay was enhanced by applying an exponential function which yielded a 50-Hz line broadening of the spectra. To analyze for the existence of non-bilayer packed phospholipids in isolated mitochondria or multilamellar liposomes, the saturation of the lamellar phase high-field resonance signal was achieved by applying a DANTE pulse train as previously described [30]. For ^{31}P-NMR assays, mitochondrial samples and multilamellar liposome samples for each experiment were prepared twice, and the integral intensity measurements of ^{31}P-NMR signals were performed three times for each sample. The technical variation between measurements was observed to be less than 8% for mitochondrial samples while the technical variation for multilamellar liposome samples was observed to be less than 5%.

^{1}H-NMR spectra from sonicated unilamellar liposomes containing the shift reagent, potassium ferricyanide $K_3[Fe(CN)_6]$, and treated with vehicle control, with DCCD-BPF or cardiotoxin CTII, were recorded at 15°C at an operating frequency of 200 MHz. The width of the 90° pulse was 8.7 μs, the relaxation delay was 50 μs, and the acquisition time for free induction signal was 1 s. The measurements of the integral intensity of ^{1}H-NMR signals from the $N^+(CH_3)_3$ groups of PC were done in triplicate readings. The variation between the triplicates was observed to be less than 6%.

To analyze the ability of CTII or DCCD-BPF for associating with individual phospholipids (CL, PA, PS or PA), the ^{31}P-NMR spectra of phospholipids in the protein-phospholipid complexes (Fig. 5a and b) were recorded at 15 °C by employing a Bruker AM-300 spectrometer (Germany) operated at a frequency of 121.5 MHz with the Bruker 10-mm multinuclear probe head tuned for ^{31}P and spin frequency at 17 cycles per s. The proton free induction decay from the sample solutions was used to adjust a field homogeneity. Proton broad-band decoupling was performed by continuous irradiation with the 90° pulse set at a pulse width 13 μs, a power of 20 kHz, and the delay between pulses of 8 s. In addition, a 2-Hz Lorentzian line-broadening function was employed to the total free induction decays to enhance the signal to noise ratio. Each sample in this study set was prepared three times and the integral intensity measurements of ^{31}P-NMR signals were performed at least three times for each sample. The variation between measurements was observed to be less than 5% across experiments.

2.6 Molecular Docking Studies

To analyze the interaction of cardiotoxin CTII, or of DCCD-BPF, with CL, the complete structure of CL (ligand) were docked with the solution NMR structure of CTII (PDB ID: 1CB9) or of DCCD-BPF (receptor) by using the AutoDockVina Version 4.2 program [31]. The PDB coordinates of CL were extracted from the bovine heart oxidoreductase crystal structure bound to CL (PDB ID: 1V54). The overall charges of CL were checked and their energies were minimized using AutoDock. The phospholipid “ligands” contained rotatable bonds whereas cardiotoxin CTII or DCCD-BPF (PDB ID: 3U32) was kept as a rigid molecule for each run. Unlike bovine DCCD-BPF, the yeast C10 subunit crystal structure (PDBID:3U32) was selected given that the coordinates of this structure were solved at high

resolution (2Å) and represent the functionally open form of the C subunit at a low pH (5.5), which facilitates proton loading and release. It is worth noting that yeast and bovine DCCD-BPF are structurally similar in amino acid sequence and show high structural homology. Therefore, this crystal structure was ideal for our docking studies based on our hypothesis CL binds the open state of the C subunit at a high concentration of H^+. In addition, the overall molecular surface of CTII or DCCD-BPF was considered for these docking studies (blind docking). A grid box for CTII was set up with following dimensions: center of x = 0.271; center of y = 0.855; center of z = 0.382; length of x = 100Å; length of y = 104Å; length of z = 104Å. A grid box for DCCD-BPF was set up with following dimensions: center of x = 35.489; center of y = 14.596; center of z = 23.144; length of x = 74Å; length of y = 70Å; length of z = 126Å. It is important to note that the grid box was large enough to perform a “blind” dock by covering the entire surface of the cardiotoxin CTII or DCCD-BPF, and a phospholipid “ligand” for each molecular docking simulation. The non-bilayer phase of a biomembrane, is significantly more hydrated than the bilayer phase which is predominantly hydrophobic in its core, and hydrophilic on both surfaces [32]. To this end, in order to simulate the biochemical environment of non-bilayer structures, the molecular simulations were done in a hydrated system (containing water molecules) at pH 7.4 to allow for electrostatic interactions. The methodology for performing molecular docking using AutoDock has been previously in our other studies for discovering CL-binding sites in mitochondrial-targeted proteins [22, 33]. Following each Autodock run, the best nine docked conformations were analyzed for ionic, ion-polar, and hydrogen bond interactions between phospholipid polar head groups and charged and polar amino acid residues of cardiotoxin CTII or DCCD-BPF by using Python Molecular Viewer (MGL Tools, The Scripps Research Institute).

3.0 Results

3.1 Non-bilayer structures can occur in mitochondria under physiological conditions

We have previously shown that certain biophysical conditions drive the formation of non-bilayer structures in intact mitochondria, an event that is associated with increased mitochondrial ATP levels [34]. Here, we now hypothesize that CL binds to ATP synthase to facilitate the formation of non-bilayer structures at the IMM that serve to increase the pool of protons that can shuttle through ATP synthase complex to enhance ATP synthesis.

Under physiological conditions, we have previously shown that the phospholipid bilayers of isolated mitochondria predominantly consist of a mobile lamellar phase interspersed with a small fraction of non-bilayer structures containing both mobile and immobilized phospholipids. Consistent with our previous study [22], we observed that proton-decoupled ^{31}P-NMR spectra from isolated mitochondria recorded at 8 °C contained an asymmetrical shaped peak located at the high-field side (Fig. 1, bottom spectra). This ^{31}P-NMR spectrum line-shape corresponds to an anisotropic orientation of phosphodiester bonds of phospholipids in a lamellar phase, a bilayer lipid organization that is present in most biological membranes [35]. In addition, this ^{31}P-NMR spectrum line-shape is consistent with mitochondria containing intact phospholipid bilayers (OMM and IMM). To determine whether ^{31}P-NMR signals associated with a non-lamellar phase (which could be caused by

small mitochondrial fragments and/or sub-mitochondrial particles) are “masked” by the lamellar phase signal, we applied a DANTE train of saturation pulses at the high-field peak of the lamellar spectrum (Fig. 1, see arrow with letter S). Following this procedure, we observed the complete disappearance of the lamellar signal, with the exception of a remnant signal (Fig. 1, horizontal hatched line). These observations suggest that most of the phospholipids from isolated mitochondrial fractions are packed as a lipid bilayer at 8 °C, likely indicating that mitochondria have normal structural integrity. In addition, the ^{31}P-NMR spectrum from isolated mitochondrial fraction recorded at 15 °C showed two small additional signals, termed signal A and B, that are superimposed on top of the lamellar signal (Fig. 1, broken vertical line is drawn at the resonance frequency of signal B). A narrow peak of signal A located at the 0 ppm frequency is associated with the presence of non-bilayer packed phospholipids of rapid isotropic molecular mobility (1×10^{-2}–10^{-4} s) [36]. In addition, a broader signal B located next to signal A is also associated with non-bilayer lipid structures but composed of phospholipids of restricted mobility [32]. To investigate whether phospholipids responsible for signals A and B exchange with phospholipids of a lamellar phase, we exposed the same isolated mitochondrial sample to a DANTE train of saturation pulses. This procedure resulted in a complete elimination of the lamellar signal and signal A. This observation suggests that phospholipids associated with the signal A efficiently exchange with phospholipids of a lamellar phase. On the other hand, signal B in the ^{31}P-NMR spectra was not affected after applying the DANTE train of saturation (Fig. 1, hatched line spectrum at 15 °C). These observations suggest that non-bilayer packed phospholipids responsible for signal B do not exchange with a lamellar phase, presumably as a consequence of the strong interaction of these phospholipids with mitochondrial membrane proteins [22]. Moreover, elevating the temperature from 15°C to 37°C resulted in a parallel increase in both populations of non-bilayer packed phospholipids associated with signals A and B in isolated mitochondrial fractions. Interestingly, an additional increase in temperature (from 37 to 43 °C) enhanced ^{31}P-NMR signal A, but did not affect the intensity of signal B (Fig. 1). Our results suggest that mitochondria contain a significant portion of non-bilayer structures under physiological conditions (37°C).

Next, we quantitatively estimated the percentage of non-bilayer immobilized phospholipids by calculating the area under the curve below the “saturated” signal B that remained after applying a train of DANTE saturation pulses (Fig. 1, hatched lines). In brief, we observed that the percentage of non-bilayer immobilized phospholipids increased from 15 °C to 37 °C, but plateaued at 43 °C (Fig. 1). Regression analyses of the data shown in figure 1 suggest that the amount of non-bilayer immobilized phospholipids are strongly correlated with the levels of mitochondrial ATP (Pearson’s coefficient= 0.97, Online supplementary material figure 1a).

In addition, we also monitored ATP synthase-driven ATP levels by measuring the mitochondrial ATP levels (also known as ATP content) from aliquots taken from the same isolated mitochondrial samples analyzed by ^{31}P-NMR. In brief, we observed that isolated mitochondrial fractions that contained a higher percentage of non-bilayer immobilized phospholipids correlated with higher ATP content when the temperature of the sample was gradually increased (8–37°C). On the other hand, the ATP levels were significantly decreased in mitochondrial fractions incubated at 43 °C, while the percentage of non-bilayer

phospholipids of immobilized mobility remained the same (Fig. 1). It is conceivable that a partial reduction in ATP levels in mitochondrial fractions incubated at 43°C is due to a robust increase in the population of non-bilayer packed phospholipids (NMR signal A) of rapid isotropic mobility resulting in the disruption in the integrity of mitochondrial membranes. However, another explanation for this result is that a decrease in ATP levels could have been due to structural perturbations in ATP synthase active centers caused by partial denaturation (suboptimal enzyme activity) at 43°C. Alternatively, beyond the ATP synthase, it is also conceivable that low (<15°C) or high temperatures (>37°C), which are outside the Arrhenius range, can affect other components of the oxidative phosphorylation pathway that may become limiting to ATP synthesis. However, if only the data that falls within the Arrhenius range of temperature is considered, there is a strong correlation of the amount of non-bilayer, immobilized phospholipids with ATP levels in mitochondria (Pearson's coefficient= 0.99, online supplementary figure 1A).

The dicyclohexylcarbodiimide (DCCD)-binding protein (DCCD-BPF, which is a part of C10 in yeast or C8 subunit in bovine) is a hydrophobic component of the F_0 sector imbedded in the IMM that is directly involved in shuttling of protons through the F_0 sector [11]. We then hypothesized that DCCD-BPF F_0 sector, or similar mitochondrial-targeted proteins, can facilitate the formation of non-bilayer structures in the IMM to stimulate ATP synthase-driven ATP levels. To this end, we examined effects of exogenous DCCD-BPF and of the cobra venom cardiotoxin CTII - a protein that favors the formation of non-bilayer structures in mitochondria [37]- on ATP levels and on the organization of phospholipids in mitochondrial membranes. In brief, we observed that treating isolated mitochondria with CTII at 15 °C enhanced both the amplitude of ^{31}P-NMR signal B (immobilized non-bilayer structures) and mitochondrial ATP levels (Fig. 2b) compared to untreated mitochondrial samples (Fig. 2a). This result suggests that increased formation of non-bilayer structures is associated with increased ATP levels. In addition, we measured mitochondrial ATP levels in mitochondria treated with 9×10^{-4} M cardiotoxin I (CTI), a cardiotoxin from *Naja naja oxiana* that has a similar three-fingered domain and high amino acid homology (80%) as CTII but that shows reduced binding to CL and a decreased ability to form non-bilayer structures in mitochondria [22]. Indeed, treating mitochondria with CTI showed a 16% decreased ability to elevate the percentage of immobilized non-bilayer structures (11.03 ±0.37% of non-bilayer structures) and a concomitant 16% reduction in ATP levels (1.68 ± 0.06 μmol/ μg, Online Supplement Figure 1B) in mitochondria incubated at 15 °C compared to CTII-treated mitochondria (1.99 ±0.070 μmol/ μg ATP, 12.97 ±0.33 % of immobilized, non-bilayer structures, figure 2). Hence, by using two cobra venom cardiotoxins that possess different non-bilayer forming activities and binding affinities to CL [22], our data provides further evidence that the formation of non-bilayer structures is highly correlated to ATP levels in mitochondria. Next, to determine the extent to which non-bilayer structures contribute to ATP levels, we analyzed the effects of DCCD-BPF and cardiotoxin CTII on mitochondrial samples in the absence and presence of cobra venom PLA_2, an enzyme that increases fluidity and non-bilayer packing of phospholipids in biological membranes [37, 38] by increasing the population of phospholipids with a rapid isotropic mobility responsible for ^{31}P-NMR signal A [39], and whose activity is synergistically enhanced by cardiotoxin CTII [37–39]. Adding PLA_2 to mitochondrial fractions pre-treated

with CTII resulted in a significant increase in the amplitude of ^{31}P-NMR signal A, a concomitant reduction of signal B, and a threefold decrease in mitochondrial ATP levels (Fig. 2c) that was markedly lower than untreated mitochondria (Fig. 2a). Hence, these results suggest that immobile non-bilayer structures contribute to both baseline and induction of ATP synthase activity. Importantly, these results suggest that increasing the levels of ^{31}P-NMR signal B is causally linked to an increase in ATP synthase activities of isolated mitochondrial fractions (non-bilayer structures directly regulate ATP levels). Furthermore, regression analyses of the data shown in figure 2 suggest that the percentage of non-bilayer immobilized phospholipids are strongly correlated with mitochondrial ATP levels (Pearson's coefficient= 0.97, Online supplementary material figure 1b). In addition, the ATP synthase activity is produced via the ATP synthase complex as treating isolated mitochondrial samples with the oligomycin (1μM), an irreversible inhibitor of the ATP synthase complex, completely abolished ATP synthesis (data not shown). Therefore, mitochondrial ATP levels shown in figure 1 are generated via the ATP synthase.

The F_0F_1 complex of the ATP synthase has been shown to form a tight association with CL [39]. We have previously shown that exogenous CTII is targeted to mitochondria to bind with CL in order to facilitate the formation of non-bilayer structures [19]. Given that both CTII and DCCD-BPF share some physico-chemical properties (e.g. hydrophobic core and a cationic molecular surface containing basic residues) and can localize to mitochondria, we then examined whether DCCD-BPF shares an intrinsic ability to actively form non-bilayer structures in mitochondria when added in an aqueous environment as CTII. Treating isolated mitochondrial fractions at 15 °C with exogenous DCCD-BPF had no effect on either the ^{31}P-NMR spectra or mitochondrial ATP levels of isolated mitochondrial fractions (Fig S1a). Adding PLA_2 to isolated mitochondrial fractions that were pre-treated with exogenous DCCD-BPF caused a small increase in the amplitude of the ^{31}P-NMR signal A and a modest decrease in mitochondrial ATP levels at 15 °C (Fig S1b) while the amplitude of ^{31}P-NMR signal B, that remained after applying the DANTE saturation pulses, was not changed (data not shown). Similar results were observed in mitochondrial fractions treated with PLA_2 in the absence of DCCD-BPF. Hence, these results suggest DCCD-BPF has no effect on PLA_2 activity or that DCCD-BPF does not interact with mitochondrial membranes when added from aqueous solution.

3.2 The F_0 subunit of the ATP synthase complex facilitates the formation of non-bilayer structures

DCCD-BPF is predominantly hydrophobic. Hence, an inability of DCCD-BPF to interact with mitochondria in an aqueous environment could be due to the predominantly hydrophobic molecular surface of DCCD-BPF [14], which is unable to interact with the polar head groups of lipids or with polar proteins at the mitochondrial surface. In contrast, CTII, despite having extensive hydrophobic areas as DCCD-BPF, is able to penetrate mitochondrial membranes to induce the formation of non-bilayer structures [22], presumably due to the presence of hydrophilic loops within the three fingered domain which can permeate mitochondrial membranes. We then surmised that DCCD-BPF does not permeate the IMM in an aqueous environment. To test this hypothesis, we performed ^{1}H-NMR analysis of sonicated unilamellar liposomes in a hydrophilic buffer containing

potassium ferricyanide $K_3[Fe(CN)_6]$, in the presence or absence of cardiotoxin CTII or DCCD-BPF, a technique used to determine whether certain proteins can penetrate the outer and inner leaflets of phospholipid membranes of unilamellar liposomes. In brief, unilamellar liposomes were made of PC, PA, PS, and CL at a molar ratio 6.5, 0.6, 0.4 and 2.5, respectively, a phospholipid composition that is similar to that of the IMM [40]. Under basal conditions, the interaction of $[Fe(CN)_6]^{-3}$ with the $N^+(CH_3)_3$ groups of PC molecules on the outer leaflet of the liposomes shifts the ^{1}H-NMR signal towards a higher magnetic field (Fig. 3, right ^{1}H-NMR signal in spectra a and d). The smaller signal is derived from the $N^+(CH_3)_3$ groups of phospholipids of the inner leaflet that is not shifted given that $[Fe(CN)_6]^{-3}$ cannot gain entry inside intact lipid membranes. These results suggest that the paramagnetic ion $[Fe(CN)_6]^{-3}$ does not permeate lipid bilayers of intact unilamellar liposomes (Fig. 3a and d) as previously reported [41]. Treating unilamellar liposomes with low concentrations of cardiotoxin CTII does not affect the signal associated with the inner leaflet (Fig. 3, b–g) indicating that $[Fe(CN)_6]^{-3}$ ions do not permeate to the inner leaflet of liposomes and that the structural integrity of phospholipid membranes remained intact. At the same time, a new ^{1}H-NMR signal was observed on the high-field side of the ^{1}H-NMR signal from the outer leaflet. This signal is more resolved on the right side of the outer leaflet signal in liposomes treated with higher concentrations of CTII (Fig. 3f and g), and is likely generated as a result of a closer distance between $[Fe(CN_6)]^{-3}$ ions and choline groups of PC lipids. This ^{1}H-NMR high-field resonance signal was first observed in our earlier work and correlated with the formation of non-bilayer structures induced by CTII. The formation of non-bilayer structures by CTII was also corroborated by using other biophysical techniques [32, 41]. This ^{1}H-NMR signal is derived from CTII-induced inverted micelles, which contain CL and PC molecules. In addition, the CTII-induced inverted micelles in PC membranes enriched with PS and/or PA, but not with CL, do not contain PC molecules [42]. The mechanism of formation of CTII-induced inverted micelles responsible for the high-field ^{1}H-NMR signal and ^{31}P-NMR signal B was previously described [42]. In contrast, DCCD-BPF did not affect the line-shape of ^{1}H-NMR signal of sonicated liposomes (Fig. 3e), suggesting that DCCD-BPF is unable to interact with biological membranes in the aqueous environment.

We then surmised that DCCD-BPF can penetrate biological membranes in a hydrophobic environment. To this end, we examined the effects of DCCD-BPF and CTII on the packing and dynamics of phospholipids in multilamellar liposomes prepared in a chloroform/methanol solution, followed by the removal of the organic solvent and by hydrating the dried lipid-protein film. The phospholipid composition of multilamellar liposomes contained PC, PA, PS, and CL at a molar ratio 6.5, 0.6, 0.4 and 2.5, respectively, a phospholipid composition that also resembles the IMM [40]. In brief, ^{31}P-NMR analyses of multilamellar liposomes in the absence of DCCD-BPF or cardiotoxin CTII exhibited a line-shape typical to phospholipids found in a lamellar phase at pH 7.4 (Fig. 4a). In further support of this concept, applying a DANTE train of saturation pulses at the high-field peak of the lamellar spectrum (see arrow with letter S in Fig. 4a) resulted in a complete elimination of the lamellar ^{31}P-NMR signal suggesting that all phospholipids in the multilamellar liposomes are organized in a bilayer structure. In addition, preparing multilamellar liposomes with a mixture of DCCD-BPF and phospholipid in a hydrophobic solvent (Fig. 4b) generated two

types of non-bilayer organized phospholipids as evident by the presence of ^{31}P-NMR signal A (phospholipids of rapid isotropic mobility) and signal B (phospholipids of immobilized mobility and with an isotropic orientation of phosphodiester bonds. Applying a DANTE pulsed train eliminated both the lamellar signal and ^{31}P-NMR signal A, with the exception of a small amount of ^{31}P-NMR signal B (see a hatched line in Fig. 4b). This observation suggests that DCCD-BPF can be incorporated into multilamellar structures and can remodel membranes by forming non-bilayer structures in a highly hydrophobic environment. Secondly, immobilized phospholipids responsible for signal B do not exchange with phospholipids of a lamellar phase, presumably due to their attraction to DCCD-BPF, whereas phospholipids responsible for signal A do not interact with DCCD-BPF and likely exchange with phospholipids of a lamellar phase. Similar results were obtained in multilamellar liposomes treated with cardiotoxin CTII (Fig. 4c), with the exception that ^{31}P-NMR signal A derived from multilamellar liposomes treated with CTII was slightly more resolved compared to multilamellar liposomes containing DCCD-BPF.

3.3 Increasing the concentration of H^+ in the IMM favors the formation of non-bilayer structures

We then surmised that increasing the concentration of protons can enhance the formation of non-bilayer structures by affecting the state of hydration and the charge and/or dipole moment of the membrane lipid polar heads, a step required for the formation of non-bilayer structures [22]. Indeed, ^{31}P-NMR spectra derived from multilamellar liposomes at pH 3.0, in the absence of DCCD-BPF or cardiotoxin CTII, contained two signals associated with lamellar phase of phospholipids: 1) a narrow signal A at 0 ppm derived from phospholipids of high isotropic mobility, and 2) an asymmetric signal derived from phospholipids organized in a lamellar phase (Fig. 4d). Applying a DANTE train of saturation pulses at the high-field peak at arrow S (Fig. 4d) resulted in a complete elimination of both signal A and the lamellar signal. This result suggests that reducing the pH increases the formation of non-bilayer structures comprised of isotropic-rapidly moving phospholipids that freely exchange with the phospholipids that exist in a lamellar phase. Treating multilamellar liposomes with DCCD-BPF or CTII generated non-bilayer structures containing immobile and mobile phospholipids within mutilamellar liposomes at a pH of 3.0: (^{31}P-NMR signals A and B) (Fig. 4e–f). The percentage of immobilized non-bilayer phospholipids induced by both proteins was higher at pH 3.0 than in multilamellar liposomes incubated at pH 7.4. These results suggest that a high concentration of H^+ and DCCD-BPF cooperate to enhance the formation of non-bilayer structures in model membranes simulating the IMM. In addition, these results suggest that DCCD-BPF and cardiotoxin CTII, when inserted into membrane environment, share similar physico-chemical properties that allow them to promote the formation of non-bilayer structures.

3.4 The F_0 sector of ATP synthase forms stable oligomeric structures by interacting with CL

The tight association of certain mitochondrial phospholipids with the F_0F_1 complex of the ATP synthase complex has been previously studied [43]. In brief, Eble et al., [43] showed that the ATP synthase complex binds to CL with a higher binding affinity compared to other mitochondrial phospholipids as determined by employing an elegant ^{31}P-NMR technique as

further described. Eble et al. employed low phospholipid concentrations in aqueous solution with 1% Triton X-100 which facilitated the formation of tiny mixed micelles made of Triton X-100 and phospholipids resulting in a high isotropic dynamics which yields narrow ^{31}P-NMR signals. A restriction of the movement of phospholipids in tiny micelles, presumably due to interactions with proteins, greatly broadens the ^{31}P-NMR signal and renders restricted phospholipids “invisible” to NMR. The disruption of a protein-phospholipid interaction by treatment with SDS liberates the restricted phospholipids and restores the ^{31}P-NMR signal. To this end, we used similar ^{31}P-NMR spectroscopy techniques to investigate whether specific mitochondrial phospholipids (PC, PA, PS, and CL) can bind tightly to DCCD-BPF in the presence of 1% Triton X-100 solution (10 mM Tris-HCl, pH 7.5, 0.5 mM EDTA, 1% Triton X-100). In brief, we observed that DCCD-BPF in the presence of 1% Triton X-100 solution did not render PC, PA or PS invisible to ^{31}P NMR spectroscopy suggesting that DCCD-BPF does not bind tightly to these phospholipids (data not shown). On the other hand, a 1% Triton X-100 solution containing DCCD-BPF, CL, and PC (1:4:7 molar ratio) rendered CL molecules invisible to ^{31}P-NMR spectroscopy while the ^{31}P-NMR signal from PC was observed (Fig. 5a). These results suggest that one mole of DCDD-BPF tightly immobilizes 4 moles of CL. Increasing the amount of exogenous CL to each sample containing DCCD-BPF, in the presence of 1% Triton X-100 solution, increased the ^{31}P-NMR signal specific for CL whereas the amplitude of the ^{31}P-NMR signal associated with PC remained relatively constant (Fig. 5a). In addition, a mixture of CL to DCCD-BPF (9 to 1 ratio) in the presence of 1% SDS treatment led to an enhancement of the ^{31}P-NMR signal specific for CL (Fig. 5a), presumably as a consequence of the 4 moles of CL released from the denatured DCCD-BPF into solution. By using the ^{31}P-NMR signal specific for PC as an internal standard, we calculated that approximately 4 moles of CL were tightly bound to one mole of DCCD-BPF. We then incubated DCCD-BPF and CL in a buffer (10 mM Tris-HCl, pH 7.5, 0.5 mM EDTA, 1% Triton X-100) free of SDS for one hour at 15 °C, and estimated the molecular weight of this protein-CL complex by performing Native PAGE assays (Fig 5c). We observed that the DCCD-BFP/CL complex was approximately 54 kDa which is consistent with a molecular weight of complex comprised of four DCCD-BPF molecules and 16 CL molecules (1 DCCD-BPF bound per 4 CL molecules). This observation suggests that incubating DCCD-BPF with CL favors the oligomerization of DCCD-BPF. On the other hand, incubating DCCD-BPF with PC, PA or PS for one hour at 15 °C did not promote the oligomerization of this DCCD-BPF (data not shown) nor it bound tightly to each of the aforementioned phospholipids.

Similarly, we analyzed the ability of PC, PA, PS, and CL to bind to CTII by using similar ^{31}P-NMR approaches. Like the DCCD-BPF, we observed that cardiotoxin CTII in 1% Triton X-100 solution does not render PC, PA or PS ^{31}P-NMR -invisible (data not shown). In addition, treating cardiotoxin CTII with 1% Triton X-100 in the presence of CL, and PC in a molar ratio of 1:4:7 respectively rendered CL undetectable by ^{31}P-NMR whereas PC was detectable by ^{31}P-NMR (Fig. 5b). Increasing the amount of exogenous CL to each sample resulted in an enhancement of the ^{31}P-NMR signal associated with CL. However, denaturing the CTII–CL complex with 1% of SDS resulted in a further increase in a visible peak of ^{31}P-NMR signal associated with the release of tightly bound CL (Fig. 5b). Based on these results, we calculated that approximately 4 moles of CL was tightly

associated with one mole of CTII. Next, we incubated CTII and CL in a buffer solution (10 mM Tris-HCl, pH 7.5, 0.5 mM EDTA, 1% Triton X-100) free of SDS for one hour at 15 °C. We then assessed the molecular weight of this protein–lipid complex by performing Native PAGE assays (Fig. 5c). By using this technique, we observed that the CTII–CL complex was approximately 50kDa, consistent with a complex comprised of 4 CTII molecules and 16 CL molecules (a ratio of one CTII molecule bound to 4 CL molecules). Like the DCCD-BPF, incubating CTII with PC, PA or PS for one hour at 15 °C did not induce the oligomerization of CTII (data not shown).

For the first time, our results suggest that CL similarly binds to DCCD-BPF or cardiotoxin CTII to induce the formation of stable lipid-protein oligomers at a stoichiometric ratio of 4 to 1. Interestingly, other phospholipids, PC, PA or PS, do not promote the oligomerization of either of these two proteins. In addition, our results suggest that the molecular surfaces of DCCD-BPF and cardiotoxin CTII share physico-chemical properties that allows them to interact with CL.

3.5 Molecular docking studies identified phospholipid binding sites in DCCD-BPF

To identify CL binding sites and elucidate molecular mechanisms by which CL interacts with DCCD-BPF, we performed molecular docking studies by using similar *in silico* approaches as previously published [22]. DCCD-BPF imbeds into the IMM by making extensive contacts with the alkyl chains of IMM phospholipids. To this end, we used the complete structure of CL (phospholipid head group plus alkyl chains) as a template (ligand) and the crystal structure of DCCD-BPF to identify CL binding sites in DCCD-BPF by using the AutoDock software. Likewise, we used the solution NMR structure of CTII to identify CL binding sites in CTII.

The molecular docking of CL to DCCD-BPF or CTII performed by AutoDock software produced nine docked conformations for each of the two proteins. The Supplemental Tables 1 and 2 describe the affinities of each binding sites in kcal/mol and list the chemical groups of the polar head of CL involved in the interaction with the basic and/or polar groups of amino acid residues of each “receptor” (DCCD-BPF or CTII), bond types, and the orientation of the head group of CL. The affinity values for each of the CL binding sites represent amount of energy released/lost when one mole of CL binds to one mole of protein. A lower energy value represents a higher binding affinity for each complex. CL binds with higher affinity to molecular surface of DCCD-BPF (affinity values −4.1 to −3.9 kcal/mol) compared to the molecular surface of CTII (affinity values −3.6 to −3.2 kcal/mol). It should be noted that the binding of CL to CTII involves more ionic, ion-polar and hydrogen bonds compared to DCCD-BPF, which predominately binds CL via weaker hydrophobic bonds (Suppl. Tables 1 and 2). Therefore, the alkyl chains of CL make broader contacts with the hydrophobic regions on the DCCD-BPF surface relative to the hydrophobic regions of CTII. Thus, our docking data suggest that a multitude of Van der Waals forces predominantly mediate the binding of CL to DCCD-BPF as opposed to ionic, ion-polar and hydrogen bond interactions, which facilitate the interaction of CL with CTII. Hence, the DCCD-BPF/CL complex releases more energy compared to the binding of CL to CTII which involves more ionic, ion-polar and hydrogen bonds, but less hydrophobic interactions. This observation is

consistent with the fact that CTII contains more basic and polar amino acid residues relative to DCCD-BPF.

Molecular docking analysis revealed that CL can bind to two types of molecular regions within the DCCD-PBF surface: 1) at the central hydrophobic region, and 2) at the polar ends of DCCD-PBF. Within the molecular surface of CTII, CL can bind to three molecular regions, two of them located at the core region and another CL binding site is located towards the edge of the molecule. All of these three molecular regions include basic, polar and non-polar amino acid residues which facilitate ionic, ion-polar, and hydrogen interactions with the CL. It should be noted that most of the CL binding sites for either DCCD-PBF or CTII share one striking similarity: the binding of CL to either protein involves at least one charged or polar moiety of the polar head of CL that is oriented away from the protein molecular surface (Fig. 6). Indeed, all nine docked conformations of CL +DCCD-PBF, and eight out of nine docked conformations of CL+CTII, revealed that charged and/or polar groups of the CL polar head are oriented towards the solution (Suppl. Tables 1 and 2), presumably to interact with neighboring proteins including additional DCCD-PBF or CTII molecules. Hence, this molecular event may explain how CL induces the oligomerization of DCCD-PBF or CTII and its ability to associate with ten c subunits found in the F_0 complex.

4.0 Discussion

4.1 Anionic phospholipids play a role in facilitating translocation of protons to the ATP synthase complex

The molecular mechanism by which protons translocate through the F_0 has been well characterized. Based on the recent high resolution X-ray crystal structural data, the F_0 sector is comprised of c subunits (8 c subunits in bovine or 10 in yeast ATP synthase) radially arranged around the stalk structure. Glu 59 within the c subunits of the F_0 sector binds to a proton within the half channel opening adjacent to a stator subunit A [3, 12]. This molecular event allows the C_{10} subunits of the rotor complex to rotate in a counter-clockwise fashion in such a manner that Glu 59 faces another half channel of the pore that is oriented towards the matrix to release the proton [12]. The active form of ATP synthase complex consist of a dimer, which is formed at the apex of cristae via the interaction of a “dimerization interface”, whereas the monomer form of ATP synthase is inactive [4, 5]. Importantly, it has been shown that the apex of cristae, which contains active dimers of ATP synthase, serves as a proton trap to increase efficiency of ATP synthase activity [4]. However, the biophysical mechanisms involved in regulating the formation of proton traps to increase the efficiency of ATP synthesis remain to be elucidated. Our data suggest that non-bilayer structures, formed via the interaction of CL with C subunits of the F_0 sector, increase ATP levels in mitochondria, presumably by favoring the formation of proton traps to increase proton flow to ATP synthase as further explained below.

Indeed, since the advent of the chemiosmotic theory of oxidative phosphorylation, there have been additional physico-chemical models that have been proposed to explain how the proton motive force, the electronegative gradient and acidic lipids - which can act as H^+ carriers [1, 2] - interplay to synergize the ATP synthesis via the ATP synthase complex. For

instance, one landmark study proposed that the generation and the release of the transmembrane proton gradient occurs via the rapid flip-flop of protonated anionic lipids, or via transient channels formed at the protein/lipid interface [2]. Another study suggested that anionic lipids can serve as proton-shuttlers [44] which generate electric field gradients along the membrane surface of IMM to power the rotation of ATP synthase complex [2]. Consistent with this view, CL has been suggested to act as a proton trap by sequestering protons from the electron-transport chain via its negatively charged phospholipid head group and subsequently releasing the protons to the F_0 sector of the ATP synthase complex [44]. Another model suggests that the non-bilayer phase transition of cardiolipins in the IMM can be induced by reducing the pH [45]. Specifically, this model is supported by the observation that certain pharmacological agents that react with acidic lipids in the IMM, can inhibit both the synthesis and hydrolysis of ATP [46]. These studies are consistent with another study that showed that the formation of non-bilayer structures is mediated by cardiolipin and phosphatidic acid, a molecular event that is correlated with increased proton translocation activity of the F_0 sector reconstituted in liposomes [15]. CL or PE, a neutral non-bilayer phospholipid in IMM, can directly modulate oxidative phosphorylation, contribute to the inner membrane potential, and are critical for maintaining the stability of respiratory chain super-complexes [20]. Another study reported a role of CL in promoting the oligomerization of the F_0 and F_1 sectors of the ATP synthase complex [47].

Non-bilayer structures are formed in specialized microdomains within the IMM to regulate mitochondrial structure and essential mitochondrial functions [15–17]. We have previously shown that non-bilayer structures exist in intact mitochondria at physiological conditions [22, 34]. However, our study is the first to describe the type and amount of non-bilayer structures (immobile vs. mobile non-bilayers) that are generated and remodeled by CL-F_0 complexes in intact mitochondria in response to various conditions: 1) [H^+], 2) temperature, and 3) cardiolipin-binding proteins known to remodel mitochondrial membranes (e.g. CTII). In addition, we show for the first time how non-bilayer structures directly modulate ATP synthesis and provide a more complete understanding of how CL, non-bilayer structures, the proton motive force and F_0 sector of the ATP synthase interplay and cooperate to enhance oxidative phosphorylation in intact mitochondria as further explained below. However, as a consequence to the formation of non-bilayers, it is conceivable that non-bilayer structures can indirectly affect other factors/molecular players that govern oxidative phosphorylation upstream of the ATP synthase complex (proton-motive-force activities and/or H^+ permeability of the IMM) and, thereby, indirectly affect ATP levels in mitochondria treated with CTII or different temperatures. Hence, our data warrants future studies to functionally dissect the bioenergetic mechanism(s) by which other OX/PHOS complexes contribute to ATP synthesis in mitochondria in response to the formation of non-bilayer structures induced by CTII or temperature.

4.2 Non-bilayer structures in mitochondria increase the efficiency of ATP synthesis

This study and our previous studies corroborate existence of non-bilayer structures in membranes of intact mitochondrial fractions [22, 34]. Our biophysical data suggest that the occurrence of these lipid structures appear to be integral to the function and maintenance of mitochondrial membrane structure, and likely modulate ATP synthesis through the ATP

synthase complex (Fig. 1–2). In further support of this concept, ^{31}P-NMR spectra from isolated mitochondrial fractions revealed two subpopulations of non-bilayer structures: one that exhibits rapid isotropic mobility of phospholipids which freely exchange with the bilayer organized phospholipids (^{31}P-NMR signal A), and a second subpopulation of lipids of restricted (immobilized) mobility which do not exchange with the bilayer packed phospholipids (^{31}P-NMR signal B). Previously, we had shown that conditions that increased the formation of non-bilayer structures in mitochondria were associated with ATP synthase activity [34]. Here, we show for the first time that local rises in [H^+] and temperature favors the formation of a subpopulation of non-bilayer phospholipids with restricted mobility (^{31}P-NMR signal B), but not of rapid isotropic mobility. The formation of non-bilayer structures of restricted mobility directly contributes to both baseline and enhanced ATP synthase activity driven by complex II (succinate) (Fig. 2). It should be noted that ^{31}P-NMR signal B cannot be attributed to the formation of hexagonal-shaped non-bilayer structures. The ^{31}P-NMR signal derived from hexagonal phase structure contains a peak in a lower field below 0 ppm and a high-field shoulder which is not observed in the ^{31}P-NMR signal B shown in figure 1. The formation of non-bilayer structures of restricted mobility is linked to tight association of CL with DCCD-PBF, presumably at three predicted CL binding sites as determined by molecular docking analyses. However, this report warrants future studies that employs elegant biophysical techniques and molecular dynamics studies to elucidate the spatial and temporal events of how DCCD-PBF/CL complexes are assembled and form non-bilayers structures at specific “microdomains” within the IMM.

In addition, we have previously shown that phospholipids with restricted mobility bind to different mitochondrial proteins (termed proteolipids). These proteolipids can form non-bilayer packed phospholipids of restricted mobility when reconstituted into multibilayer liposomes [14]. Consistent with this model, we show here that DCCD-BPF reconstituted into multibilayer liposomes also forms non-bilayer packed phospholipids of restricted mobility (Fig. 4b) suggesting that immobile non-bilayer phospholipids are tightly bound to DCCD-BPF (the most hydrophobic protein in the F_0 sector [14]), and possibly to other proteins of the F_0 sector.

In addition, we examined the ability of individual phospholipids to associate with DCCD-BPF. Interestingly, only CL but no other anionic phospholipids, strongly associated with the DCCD-BPF of the F_0 sector. For the first time, we identified the stoichiometry of CL to DCCD-BPF complexes that form in model membranes of IMM. Specifically, one mole of DCCD-BPF tightly bound up to four moles of CL in the presence of 1% Triton X-100 solution (Fig. 5a). Moreover, increasing the concentration of protons by decreasing the pH to 3.0, increased the fraction of immobilized phospholipids (20.1%) (Fig. 4). This observation suggests that increasing the concentration of protons at the IMM space elevates the formation of non-bilayer structures in the IMM, a molecular event that is linked to an increase in ATP synthesis. Interestingly, given that DCCD-BPF forms oligomeric structures with CL, the observation that DCCD-BPF/CL complexes are recalcitrant to 1% Triton X-100 treatment suggests that CL avidly binds between two DCCD-BPFs. Based on this data, we propose that 16 CL molecules are bound to 4 protein molecules (protein to lipid ratio 1: 4).

Like DCCD-BPF, CTII can also strongly associate with CL and form oligomeric structures and induce the formation of non-bilayer structures with similar ^{31}P-NMR spectra (Fig. 5c) at a similar phospholipid to protein stoichiometric ratio (11:1 at pH 7.4, and 14:1 at pH 3.0). Hence, these observations suggest that CTII phenocopies the ability of DCCD-BPF to form lipid-protein oligomers by binding to CL, presumably due to similar physico-chemical properties of their molecular surfaces. Hence, our data suggest that the formation of non-bilayer structures, mediated by CTII or DCCD-BFP, increase ATP synthesis presumably via stabilizing the formation of active dimers of ATP synthase and possibly oligomers located at the apex of cristae junctions [4].

A minimum amount of non-bilayer immobilized phospholipids in the IMM may be important for maintaining the integrity of the IMM. Our ^{1}H-NMR studies on the effects of CTII on the permeability of unilamellar liposomes confirms the ability of CTII to induce the formation of non-bilayer structures without compromising the structural integrity (barrier properties) of model membranes with a lipid composition similar to that of the IMM (Fig. 3 b–g). However, at higher temperatures and higher concentrations, cardiotoxin CTII can increase the amount of non-bilayer structures to induce the permeabilization, and consequent lysis of the IMM, presumably by totally destroying the native organization of the lamellar phase of biological membranes [22, 24, 37, 38].

4.3 Proposed Mechanism by which the H^+ gradient generates non-bilayer structures that act as proton traps

The transition from a bilayer to non-bilayer phase in the IMM at physiological conditions could be attributed to a high concentration of local H^+ that interact with anionic phospholipids at the IMM. Indeed, pH-dependent polymorphic phase transitions of CL, in which CL contributes to the formation of a bilayer structure at neutral pH and of a non-bilayer structure at low pH, has been previously reported [46, 48]. Mechanistically, H^+ ions interact with two PO_4^- groups of CL to neutralize its negative charge and to reduce the size of the hydrate coat around the polar head of phospholipid [32]. The neutralized CL then acquires a reverse wedge molecular shape which covers less area at the surface of the polar head compared to the four alkyl chains of CL. This molecular event mediates the transition from a bilayer to non-bilayer packing of CL [36, 49], leading to the formation of specific regions containing inverted micelles near highly protonated regions of neighboring membranes. In this hypothetical inverted micelle, CL molecules are localized within highly curved areas of inverted micelles in such a way that some of the polar heads of CL are attracted to positively charged amino acid residue(s) of a membrane protein including DCCD-BPF [22, 32, 37, 39, 41, 50]. In Fig. 7, we depict a conceptual model in which a low pH induces the formation of an inverted micelle caused by the protonation of the polar heads of CL which are likely located at the apex of cristae which favors the formation of proton traps and clustering of ATP synthase dimers [3]. This hypothetical inverted micelle connects two adjacent IMM of cristae in such a manner that brings together several ATP-synthases separated by the core of the inverted micelle which serves to trap a high concentration of protons. In Fig. 7 we only depict two inverted micelles, one at the apex of cristae that includes six ATP-synthases (three dimers), and another inverted micelle adjacent to the cristae's apex that include four ATP-synthases (two dimers). The ATP synthase dimers form

an oligomeric ribbon of dimers brought together by inverted micelles, while the lipids of the cristae facilitate an assembly of ATP synthases as previously reported in another study [47]. A high H^+ concentration inside an inverted micelle core may force protons through the two halves of the F_0 channel of the ATP synthase complex, a hypothetical structure of which has been previously described [1, 12]. Furthermore, this inverted micelle connecting two adjacent IMM may be an intermediate step that facilitates membrane fusion in a similar fashion as mediated by V-ATPases [51].

Furthermore, our *in silico* docking studies revealed that CL binds to DCCD-BPF by making extensive hydrophobic interactions whereas the polar groups of the phospholipid head of CL are oriented away from the molecular surface of DCCD-BPF, presumably to interact with neighboring DCCD-PBF (Fig. 6a,b) or with C subunits of the ATP synthase complex. This mode of binding may explain how CL binds to DCCD-BPF to promote the formation of stable protein-lipid complexes in Triton X-100 solution. A high concentration of a local pool of H^+ caused by transient drops in pH in the IMM can favor the formation of inverted micelles. In this conformation, protonated CLs acquire a reverse wedge molecular shape which forces the formation of inverted micelles at protonated contacts of adjacent IMM regions, and are capable of bringing together numerous ATP synthase complexes. This molecular event is a plausible mechanism by which CL promotes the oligomerization of ATP synthase complexes and the subsequent entrapment of protons within the core of an inverted micelle to increase the efficiency of ATP synthesis. One example by which inverted micelles in the IMM may contribute to increase ATP synthesis occur in Drosophila flight-muscle mitochondria which contain cristae that are enriched in supra-molecular assemblies of ATP synthase complexes [47].

4.4 Proposed Mechanism by which Non-Bilayer Structures form toroidal-like pores in the IMM to rapidly depolarize mitochondria

We have previously shown that CTII induces the formation of toroidal-like pores in liposomes enriched with PC and either PA or PS [34, 41]. In such pores, the long molecular axis of PA and PS is positioned perpendicular to the membrane surface normal with the phospholipids polar head facing the aqueous solution while the alkyl chains of the lipids interact with the non-polar regions of CTII embedded in the membrane. Our *in silico* docking studies suggest that CTII and DCCD-PBF bind CL by employing similar types of intermolecular forces including hydrogen, ionic, and extensive hydrophobic interactions (Fig. 6). In this work, we also showed that CTII and DCCD-BPF reconstituted in multilamellar liposomes exhibit very similar levels of non-bilayer forming activities (Fig. 4) and an ability to form oligomeric lipid-protein complexes (Fig. 5). These observations suggest that the molecular surfaces of CTII and DCCD-PBF share some physico-chemical properties that enables them to bind CL, and favor the formation of non-bilayer structures in the IMM. Although *in silico* docking studies identified potential CL-binding sites in DCCD-BFP, a caveat with performing affinity docking studies is that this *in silico* technique is limited in the sense that these computer simulations are static and do not provide an overall understating of how CL-DCCD-BPF complexes can dynamically form non-bilayer structures over time within the native environment of a phospholipid bilayer. Therefore, future studies that involve performing molecular dynamic studies (coarse grained and/or all

atom dynamics) will be valuable to further understand how CL-DCCD-BPF complexes can form non-bilayer structures in computer-simulated IMM lipid bilayers.

Like CTII, it is plausible that DCCD-BPF facilitate the formation of toroidal-like pores at higher concentrations of H^+ in certain regions of the IMM, presumably in membranes of inverted micelles (between monomers of a dimer) that favor the formation of proton traps (Fig. 7) [3]. Such pores may serve to release high concentrations of H^+ from the IMM space into the matrix of mitochondria as a mechanism to rapidly depolarize mitochondria and maintain the structural integrity of the IMM when exposed to such a high concentration of H^+. There is some evidence to support this model. Indeed, by employing ^{2}H-NMR spectroscopy, we have previously shown that at low pH, a high concentration of H^+ can interact with water molecules bound to phospholipid polar heads at a local membrane region. These H^+ are immobilized by ion-polar interactions with the carboxyl and phosphate groups of PS and with a phosphate group of PA [32]. This molecular event effectively increases the surface area of the polar head of PS and PA relative to the hydrophobic area of their alkyl chains, which destabilizes the bilayer lipid packing and drives the formation of toroidal-like pores [52]. Likewise, our ^{31}P-NMR data suggest that reducing the pH of multilamellar liposomes containing DCCD-BPF (Fig. 4e, pH 3.0) increases the formation of non-bilayer structures, which may include toroidal-like pores which share a similar ^{31}P-NMR fingerprint as inverted micelles [22]. However, we acknowledge that more experimental evidence is needed to confirm the existence of toroidal pores at the IMM and to support the concept that toroidal pores in mitochondria allow protons to bypass the ATP synthase and flow into the matrix to rapidly induce mitochondrial depolarization as a way to preserve the structural integrity of the cristae.

It should be noted, that despite significant differences in the amino acid sequences between DCCD-BPF and CTII, both proteins have a common structural features within their molecular surfaces. For instance, both proteins have a predominantly hydrophobic surface area, which can presumably allow the proteins to imbed through the length of phospholipid alkyl chains of a lipid bilayer, and the presence of a molecular surface area containing charged and polar amino acid residues that can interact with polar heads of phospholipids. For DCCD-BPF, the key amino acid residue seems to be Lys-44 which makes ionic bond with one PO_4^- group of CL and leaves another PO_4^- group for possible dimerization with another DCCD-BPF (Suppl Table 1 - Binding site 5). The neutralization of both PO_4^- groups of CL by an ATP synthase dimer increases the surface curvature of IMM, possibly to allow inverted micelles formation to entrap higher concentration of H^+ ions (Fig. 7). A similar type of dimerization mechanism may occur for CTII as well (Suppl Table 2 - Binding sites 3 and 8). However, we want to emphasize that the difference between DCCD-BPF and CTII is that CTII, unlike DCCD-BPF, contains a strongly polycationic flanking region which allows CTII to penetrate a hydrophilic barrier of membranes from an aqueous solution. This molecular event may explain an increase in ATP synthase activity in response to succinate in mitochondrial samples at 15 °C treated with CTII (Fig. 2 B).

5.0 Conclusion

By using intact mitochondria and model membranes that simulate the IMM environment, our data support a model by which H^+, CLs and DCCD-BP interplay to facilitate the formation of non-bilayer structures to increase ATP synthesis. First, we propose that an increase in temperature, and a low pH at the IM space, which facilitates an increase in proton concentration, increases the formation of inverted micelles, which are predominantly composed of CL, but also include PC and possibly other acidic phospholipids. These inverted micelles may favor the formation of specialized “microdomains” to recruit oligomeric complexes conformed of F_0 and CL which serve to maintain a high concentration of protons by forming proton traps to accelerate proton translocation and subsequent ATP synthesis. Upon reaching a specific threshold of concentration of H^+ at the IM space, toroidal-like pores may form to induce a rapid decrease in the transmembrane potential by facilitating a rapid flow of protons into the mitochondrial matrix. However, our results warrants future studies to further functionally dissect the roles that non-bilayer structures (e.g. inverted micelles and toroidal-like pores) play in maintaining mitochondrial structure and function under physiological conditions and in mitochondrial-related diseases.

Supplementary Material

Refer to Web version on PubMed Central for supplementary material.

Acknowledgments

This work was predominantly supported by a start-up grant from Moscow State University (to SEG), and partly supported by a National Institute of Health (NIH) grant GM103554 (to RKD), and by a 2014 International Activities Grant Award (University of Nevada, Reno to RKD and SEG).

References

1. Nakamoto RK, Scanlon JAB, Al-Shawi MK. The rotary mechanism of the ATP synthase. Archives of biochemistry and biophysics. 2008; 476:43–50. [PubMed: 18515057]
2. Kocherginsky N. Acidic lipids, H+-ATPases, and mechanism of oxidative phosphorylation. Physico-chemical ideas 30 years after P. Mitchell’s Nobel Prize award. Progress in biophysics and molecular biology. 2009; 99:20–41. [PubMed: 19049812]
3. Watt IN, Montgomery MG, Runswick MJ, Leslie AG, Walker JE. Bioenergetic cost of making an adenosine triphosphate molecule in animal mitochondria. Proceedings of the National Academy of Sciences of the United States of America. 2010; 107:16823–16827. [PubMed: 20847295]
4. Strauss M, Hofhaus G, Schroder RR, Kuhlbrandt W. Dimer ribbons of ATP synthase shape the inner mitochondrial membrane. The EMBO journal. 2008; 27:1154–1160. [PubMed: 18323778]
5. Wittig I, Carrozzo R, Santorelli FM, Schagger H. Supercomplexes and subcomplexes of mitochondrial oxidative phosphorylation. Biochimica et biophysica acta. 2006; 1757:1066–1072. [PubMed: 16782043]
6. Habersetzer J, Ziani W, Larrieu I, Stines-Chaumeil C, Giraud MF, Brethes D, Dautant A, Paumard P. ATP synthase oligomerization: from the enzyme models to the mitochondrial morphology. The international journal of biochemistry & cell biology. 2013; 45:99–105. [PubMed: 22664329]
7. Wittig I, Meyer B, Heide H, Steger M, Bleier L, Wumaier Z, Karas M, Schagger H. Assembly and oligomerization of human ATP synthase lacking mitochondrial subunits a and A6L. Biochimica et biophysica acta. 2010; 1797:1004–1011. [PubMed: 20188060]

8. Collinson IR, Skehel JM, Fearnley IM, Runswick MJ, Walker JE. The F1F0-ATPase complex from bovine heart mitochondria: the molar ratio of the subunits in the stalk region linking the F1 and F0 domains. Biochemistry. 1996; 35:12640–12646. [PubMed: 8823202]
9. Collinson IR, Runswick MJ, Buchanan SK, Fearnley IM, Skehel JM, van Raaij MJ, Griffiths DE, Walker JE. Fo membrane domain of ATP synthase from bovine heart mitochondria: purification, subunit composition, and reconstitution with F1-ATPase. Biochemistry. 1994; 33:7971–7978. [PubMed: 8011660]
10. Giraud MF, Paumard P, Sanchez C, Brethes D, Velours J, Dautant A. Rotor architecture in the yeast and bovine F1-c-ring complexes of F-ATP synthase. Journal of structural biology. 2012; 177:490–497. [PubMed: 22119846]
11. Fillingame RH. The proton-translocating pumps of oxidative phosphorylation. Annual review of biochemistry. 1980; 49:1079–1113.
12. Symersky J, Pagadala V, Osowski D, Krah A, Meier T, Faraldo-Gómez JD, Mueller DM. Structure of the c10 ring of the yeast mitochondrial ATP synthase in the open conformation. Nature structural & molecular biology. 2012; 19:485–491.
13. Symersky J, Osowski D, Walters DE, Mueller DM. Oligomycin frames a common drug-binding site in the ATP synthase. Proceedings of the National Academy of Sciences of the United States of America. 2012; 109:13961–13965. [PubMed: 22869738]
14. Segal NK, Gasanov SE, Palamarchuk LA, Ius'kovich AK, Kolesova GM, Mansurova SE, Iaguzhinskii LS. Mitochondrial proteolipids. Biokhimiia. 1993; 58:1812–1819. [PubMed: 8268319]
15. Yang H, Huang Y, Zhang X, Yang F. Cardiolipin is essential for higher proton translocation activity of reconstituted F0. Sci China C Life Sci. 2001; 44:146–155. [PubMed: 18726431]
16. Schlame M, Acehan D, Berno B, Xu Y, Valvo S, Ren M, Stokes DL, Epand RM. The physical state of lipid substrates provides transacylation specificity for tafazzin. Nature chemical biology. 2012; 8:862–869. [PubMed: 22941046]
17. Zazueta C, Ramirez J, Garcia N, Baeza I. Cardiolipin regulates the activity of the reconstituted mitochondrial calcium uniporter by modifying the structure of the liposome bilayer. The Journal of membrane biology. 2003; 191:113–122. [PubMed: 12533778]
18. Jouhet J. Importance of the hexagonal lipid phase in biological membrane organization. Frontiers in plant science. 2013; 4:494. [PubMed: 24348497]
19. Joshi AS, Thompson MN, Fei N, Huttemann M, Greenberg ML. Cardiolipin and mitochondrial phosphatidylethanolamine have overlapping functions in mitochondrial fusion in Saccharomyces cerevisiae. The Journal of biological chemistry. 2012; 287:17589–17597. [PubMed: 22433850]
20. Böttinger L, Horvath SE, Kleinschroth T, Hunte C, Daum G, Pfanner N, Becker T. Phosphatidylethanolamine and cardiolipin differentially affect the stability of mitochondrial respiratory chain supercomplexes. Journal of molecular biology. 2012; 423:677–686. [PubMed: 22971339]
21. Haines TH, Dencher NA. Cardiolipin: a proton trap for oxidative phosphorylation. FEBS letters. 2002; 528:35–39. [PubMed: 12297275]
22. Gasanov SE, Shrivastava IH, Israilov FS, Kim AA, Rylova KA, Zhang B, Dagda RK. Naja naja oxiana cobra venom cytotoxins CTI and CTII disrupt mitochondrial membrane integrity: implications for basic three-fingered cytotoxins. PloS one. 2015; 10:e0129248. [PubMed: 26091109]
23. Grishin EV, Sukhikh AP, Adamovich TB, Yu A, Ovchinnikov A. The isolation and sequence determination of a cytotoxin from the venom of the Middle-Asian cobra Naja naja oxiana. FEBS letters. 1974; 48:179–183. [PubMed: 4435217]
24. Gasanov SE, Alsarraj MA, Gasanov NE, Rael ED. Cobra venom cytotoxin free of phospholipase A2 and its effect on model membranes and T leukemia cells. The Journal of membrane biology. 1997; 155:133–142. [PubMed: 9049107]
25. Cunningham CC, George DT. The relationship between the bovine heart mitochondrial adenosine triphosphatase, lipophilic compounds, and oligomycin. The Journal of biological chemistry. 1975; 250:2036–2044. [PubMed: 123247]

26. Rogers GW, Brand MD, Petrosyan S, Ashok D, Elorza AA, Ferrick DA, Murphy AN. High throughput microplate respiratory measurements using minimal quantities of isolated mitochondria. PloS one. 2011; 6:e21746. [PubMed: 21799747]
27. Drew B, Leeuwenburgh C. Method for measuring ATP production in isolated mitochondria: ATP production in brain and liver mitochondria of Fischer-344 rats with age and caloric restriction, American journal of physiology. Regulatory, integrative and comparative physiology. 2003; 285:R1259–1267.
28. Serrano R, Kanner BI, Racker E. Purification and properties of the proton-translocating adenosine triphosphatase complex of bovine heart mitochondria. The Journal of biological chemistry. 1976; 251:2453–2461. [PubMed: 177416]
29. Sebald W, Graf T, Lukins HB. The dicyclohexylcarbodiimide-binding protein of the mitochondrial ATPase complex from Neurospora crassa and Saccharomyces cerevisiae. Identification and isolation. European journal of biochemistry / FEBS. 1979; 93:587–599.
30. Smith, IC., Ekiel, IH. Phosphorous-31 NMR: Principles and Applications. Academic Press; Orlando, FL: 1984. Phosphorus-31 NMR of phospholipids in membranes; p. 447-475.
31. Trott O, Olson AJ. AutoDock Vina: improving the speed and accuracy of docking with a new scoring function, efficient optimization, and multithreading. Journal of computational chemistry. 2010; 31:455–461. [PubMed: 19499576]
32. Gasanov SE, Kamaev FG, Salakhutdinov BA, Aripov TF. The fusogenic properties of the cytotoxins of cobra venom in a model membrane system. Nauchnye doklady vysshei shkoly. Biologicheskie nauki. 1990:42–50.
33. Chu CT, Ji J, Dagda RK, Jiang JF, Tyurina YY, Kapralov AA, Tyurin VA, Yanamala N, Shrivastava IH, Mohammadyani D, Qiang Wang KZ, Zhu J, Klein-Seetharaman J, Balasubramanian K, Amoscato AA, Borisenko G, Huang Z, Gusdon AM, Cheikhi A, Steer EK, Wang R, Baty C, Watkins S, Bahar I, Bayir H, Kagan VE. Cardiolipin externalization to the outer mitochondrial membrane acts as an elimination signal for mitophagy in neuronal cells. Nature cell biology. 2013; 15:1197–1205. [PubMed: 24036476]
34. Gasanov SE, Kim AA, Dagda RK. The Possible Role of Nonbilayer Structures in Regulating ATP Synthase Activity in Mitochondrial Membranes. Biophysics. 2016; 61:596–600. [PubMed: 28065984]
35. Cullis P, De Kruijff B, Hope M, Nayar R, Rietveld A, Verkleij A. Structural properties of phospholipids in the rat liver inner mitochondrial membrane. A 31 P-NMR study. Biochimica et Biophysica Acta (BBA)-Biomembranes. 1980; 600:625–635. [PubMed: 7407135]
36. De Kruijff B, Cullis P, Verkleij A, Hope M, van Echteld C, Taraschi T, Van Hoogevest P, Killian J, Rietveld A, Van der Steen A. Modulation of lipid polymorphism by lipid-protein interactions. Progress in protein-lipid interactions. 1985:89–142.
37. Gasanov SE, Dagda RK, Rael ED. Snake venom cytotoxins, phospholipase A2s, and Zn2+-dependent metalloproteinases: mechanisms of action and pharmacological relevance. Journal of clinical toxicology. 2014; 4:1000181. [PubMed: 24949227]
38. Gasanov SE, Rael ED, Martinez M, Baeza G, Vernon LP. Modulation of phospholipase A_2 activity by membrane-active peptides on liposomes of different phospholipid composition. General physiology and biophysics. 1994; 13:275–275. [PubMed: 7890144]
39. Gasanov SE, Gasanov NE, Rael ED. Phospholipase A2 and cobra venom cytotoxin Vc5 interactions and membrane structure. General physiology and biophysics. 1995; 14:107–123. [PubMed: 8846880]
40. Daum G. Lipids of mitochondria. Biochimica et Biophysica Acta (BBA)-Reviews on Biomembranes. 1985; 822:1–42. [PubMed: 2408671]
41. Aripov T, Gasanov S, Salakhutdinov B, Rozenshtein I, Kamaev F. Central Asian cobra venom cytotoxins-induced aggregation, permeability and fusion of liposomes. Gen Physiol Biophys. 1989; 8:459–473. [PubMed: 2591725]
42. Gasanov SE, Salakhutdinov BA, Aripov TF. Formation of nonbilayer structures in phospholipid membrane induced by cationic polypeptides. BIOLOGICHESKIE MEMBRANY. 1990a; 7:1045–1055.

43. Eble KS, Coleman WB, Hantgan RR, Cunningham CC. Tightly associated cardiolipin in the bovine heart mitochondrial ATP synthase as analyzed by 31P nuclear magnetic resonance spectroscopy. Journal of Biological Chemistry. 1990; 265:19434–19440. [PubMed: 2147180]
44. Haines TH. Anionic lipid headgroups as a proton-conducting pathway along the surface of membranes: a hypothesis. Proceedings of the National Academy of Sciences. 1983; 80:160–164.
45. Alessandrini A, Valdrè G, Valdrè U, Muscatello U. Defects in ordered aggregates of cardiolipin visualized by atomic force microscopy. Chemistry and physics of lipids. 2007; 146:111–124. [PubMed: 17274972]
46. Tokarska-Schlattner M, Wallimann T, Schlattner U. Alterations in myocardial energy metabolism induced by the anti-cancer drug doxorubicin. Comptes rendus biologies. 2006; 329:657–668. [PubMed: 16945832]
47. Acehan D, Malhotra A, Xu Y, Ren M, Stokes DL, Schlame M. Cardiolipin affects the supramolecular organization of ATP synthase in mitochondria. Biophysical journal. 2011; 100:2184–2192. [PubMed: 21539786]
48. De Kruijff, B., Cullis, P., Verkleij, A., Hope, M., Van Echteld, C., Martonosi, TTA. The Enzymes of Biological Membranes. 2nd. Vol. 1. Plenum Press; New York: 1985.
49. Chernomordik LV, Kozlov MM. Mechanics of membrane fusion. Nature structural & molecular biology. 2008; 15:675–683.
50. Gasanov SE, Vernon LP, Aripov TF. Modification of phospholipid membrane structure by the plant toxic peptide Pyrularia thionin. Archives of biochemistry and biophysics. 1993; 301:367–374. [PubMed: 8384833]
51. Merz AJ. What are the roles of V-ATPases in membrane fusion? Proceedings of the National Academy of Sciences of the United States of America. 2015; 112:8–9. [PubMed: 25540413]
52. Wi S, Kim C. Pore structure, thinning effect, and lateral diffusive dynamics of oriented lipid membranes interacting with antimicrobial peptide protegrin-1: 31P and 2H solid-state NMR study. The journal of physical chemistry B. 2008; 112:11402–11414. [PubMed: 18700738]

Research Highlights

- Changes in pH modulate the formation of non-bilayer structures in model membranes
- Non-bilayer structures, including inverted micelles, regulate ATP synthesis
- Cardiolipin facilitates the formation of non-bilayer structures
- DCCD-binding protein of F_0 sector augments the formation of non-bilayer structures
- CL binds to the DCCD-binding protein of the F_0 sector

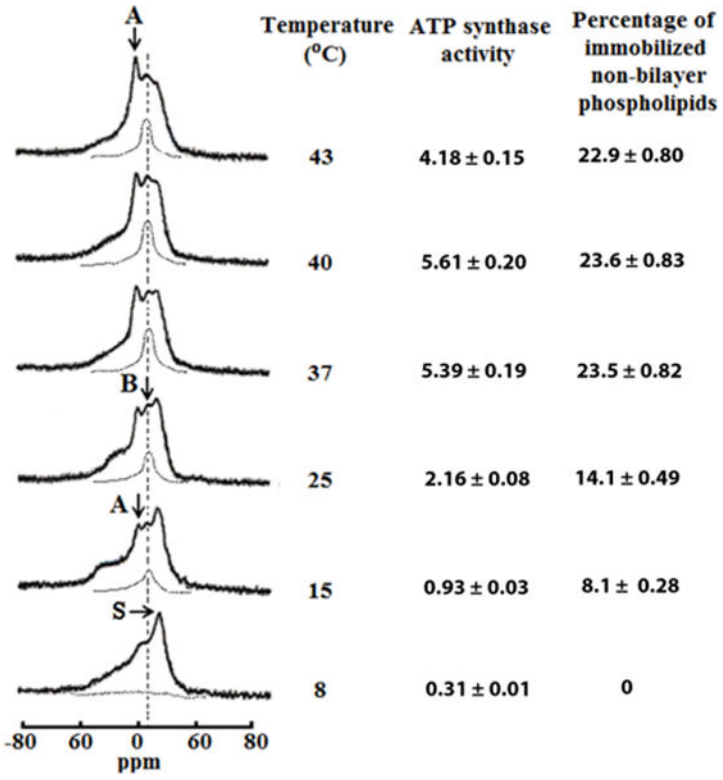

Fig. 1. Temperature affects the formation of non-bilayer structures and ATP synthase activity in mitochondria

^{31}P-NMR spectra of mitochondria recorded at various temperatures in the presence of 1.5mM succinate. The phospholipid concentration for each mitochondrial sample was estimated to be approximately 6.3×10^{-2} M, as assessed by normalizing the integral intensity of the ^{31}P-NMR signals from the mitochondrial samples to the integrated intensity of the ^{31}P-NMR signals measured from large multilamellar liposomes. Hatched lines are saturation spectra observed after applying a DANTE train of saturation pulses at the high-field peak of the lamellar spectrum (see arrow with letter S). Position of the hatched line signals in saturation spectra coincides with the position of ^{31}P-NMR signal B. The amount of non-bilayer immobilized phospholipids was estimated by calculating the area under the hatched ^{31}P-NMR lines below the signal B after a DANTE train of saturation was applied. The percentage of non-bilayer immobilized phospholipids are shown on the column on the right as means with standard errors (±SEM) compiled from three independent experiments. Statistical differences were observed between ATP synthase activity and amount of non-bilayer phospholipids in mitochondria incubated at 25 °C vs. 15°C (One Way ANOVA, Tukey's test). ATP levels expressed as μmol ATP synthesized per mg of mitochondrial proteins, was monitored by taking measurements on aliquots from the ^{31}P-NMR sample tubes. ATP levels are shown on the left column as means with standard errors (±SEM) compiled from three independent experiments. Each ^{31}P-NMR spectrum shown is representative of two independent experiments that showed similar results. Each sample was measured in triplicate readings.

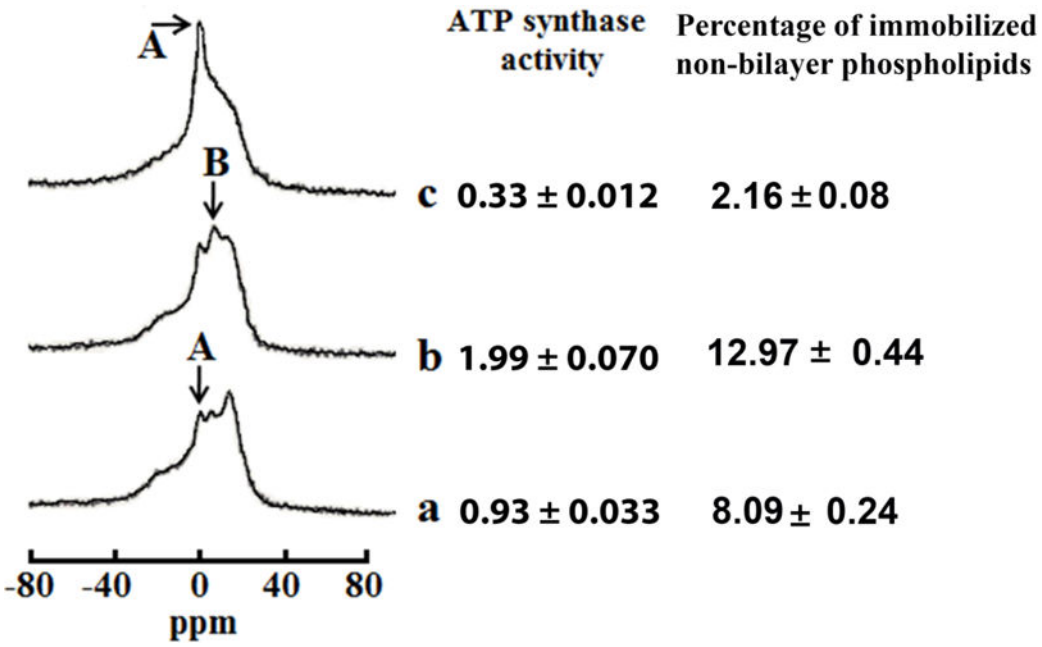

Fig. 2. Non-bilayer structures modulate ATP synthase activity in mitochondria

^{31}P-NMR spectra of mitochondria recorded in the presence of 1.5mM succinate at 15 °C in a control sample (**a**), and in the samples treated with 9×10^{-4} M CTII (**b**), pre-treated with 9×10^{-4} M CTII and post-treated with 1×10^{-7} M PLA_2 (**c**). The phospholipid concentration in each mitochondrial sample was estimated to be approximately 6.3×10^{-2} M, which was assessed by normalizing the integrated density of the ^{31}P-NMR signals from the mitochondrial samples to the integrated density of the ^{31}P-NMR signals from large multilamellar liposomes. The amount of non-bilayer immobilized phospholipids was estimated by calculating the area under the signal remained after a DANTE train of saturation was applied at the high-field peak of the lamellar spectrum (not shown). The percentage of non-bilayer immobilized phospholipids are shown on the column on the right as means with standard errors (±SEM) compiled from three independent experiments. The ATP levels, expressed as μmol ATP synthesized per mg of mitochondrial proteins, was monitored by taking measurements on aliquots from the ^{31}P-NMR sample tubes. ATP levels are shown on the right column as means with standard errors (±SEM) compiled from three independent experiments. Statistical differences were observed between ATP synthase activity in untreated mitochondria (**a**) vs. mitochondria treated with CTII (**b**) (One Way ANOVA, Fisher's LSD). Each ^{31}P-NMR spectrum shown is representative of two independent experiments that showed similar results. Each sample was measured in triplicate readings.

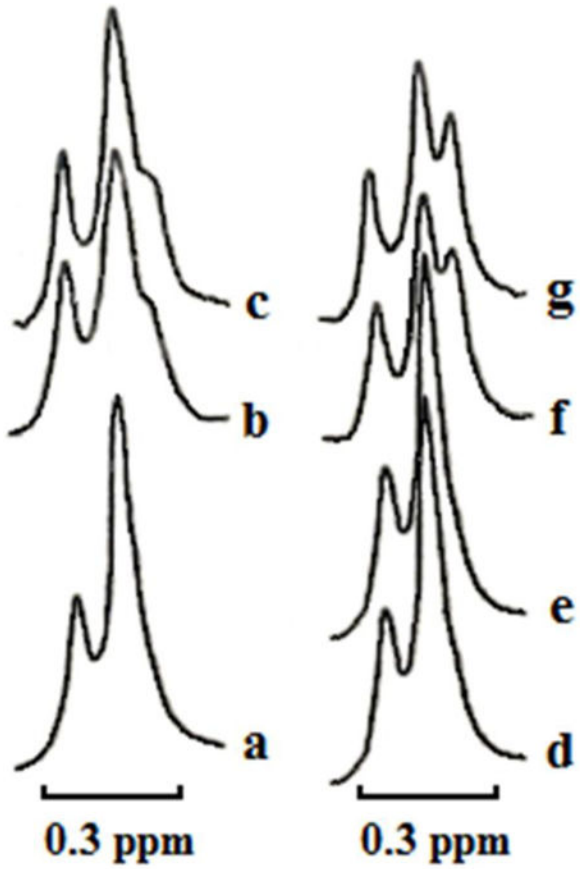

Fig. 3. CTII but not DCCD-BPF can bind to liposomes enriched in CL

^{1}H-NMR spectra derived from the $N^+(CH_3)_3$ groups of PC in sonicated unilamellar liposomes composed of PC, PA, PS and CL in molar ratio 6.5, 0.6, 0.4 and 2.5 respectively at a total lipid concentration 1.4×10^{-2} M in the presence of $K_3Fe(CN)_6$ (10 μl of saturated $K_3Fe(CN)_6$ solution per 1 ml of liposomes) at 15 °C. Control ^{1}H-NMR spectra (**a** and **d)** derived from liposomes incubated for 30 min in a tube for ^{1}H-NMR prior to adding $K_3Fe(CN)_3$. The other ^{1}H-NMR spectra were recorded from liposomes incubated with 1×10^{-4} M CTII (**b**) or 2×10^{-4} M CTII (**f**) or 2×10^{-4} M DCCD-binding protein (**e**) for 30 min prior to addition of $K_3Fe(CN)_6$. ^{1}H-NMR spectra (**c** and **g)** derived from liposome samples used in panels **b** and **f** respectively but recorded 1 hour later. Each ^{1}H-NMR spectrum shows representative ^{1}H-NMR traces from three independent experiments that showed similar results. Each sample (**a – g**) was measured in triplicate.

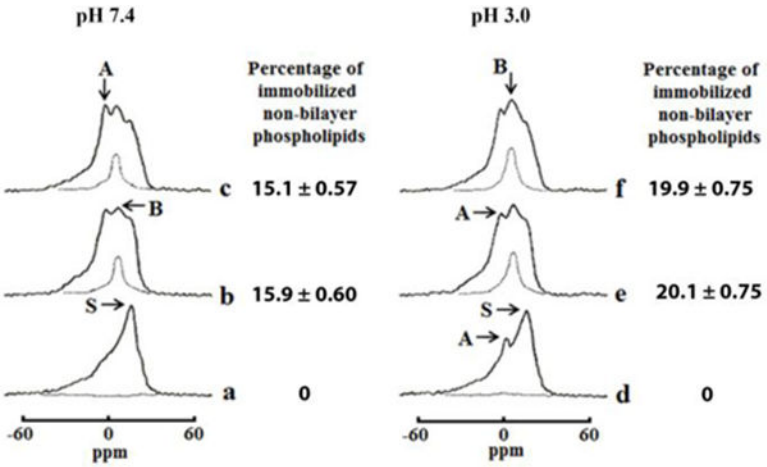

Fig. 4. DCCD-BPF and CTII reconstituted into multilamellar liposomes form greater amount of immobilized non-bilayer packed phospholipids at lower pH

^{31}P-NMR spectra from multilamellar liposomes composed of PC, PA, PS, and CL in a molar ratio 6.5, 0.6, 0.4 and 2.5 respectively at a total lipid concentration 6.3×10^{-2} M recorded at 15 °C in a buffer at pH 7.4 (**a**, **b**, **c**) or at pH 3.0 (**d**, **e**, **f**) in absence (**a, d**) or presence 9×10^{-4} M DCCD-PBF (**b, e**) or 9×10^{-4} M CTII (**c, f**). DCCD-BPF and CTII were reconstituted into a lamellar phase by mixing a protein and phospholipids in chloroform/methanol solution, evaporation of organic solvent, and hydration of a protein-lipid film as described in Materials and Methods. Hatched lines are saturation spectra observed after applying a DANTE train of saturation pulses at the high-field peak of the lamellar spectrum (see arrow with letter S). Each ^{31}P-NMR spectrum shown is representative of two independent experiments with similar results. Each sample was measured in triplicate readings. The amount of non-bilayer immobilized phospholipids was estimated by calculating the area under the hatched ^{31}P-NMR lines below the signal B after a DANTE train of saturation pulses was applied. The percentage of non-bilayer immobilized phospholipids are shown on the column on the right of the ^{31}P NMR spectra as means with standard errors (±SEM) compiled from three independent experiments.

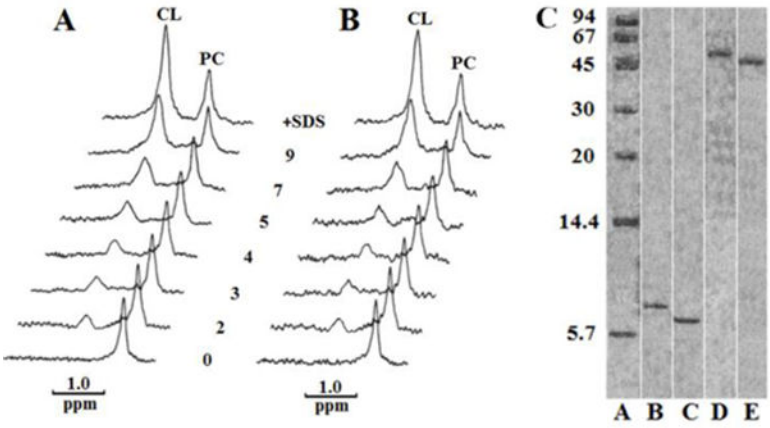

Fig. 5. CL binds avidly to DCCD-BPF and CTII

^{31}P-NMR spectra of PC and CL in preparations containing 1.2×10^{-6} M DCCD-BPF (**A**) or 1.2×10^{-6} M cardiotoxin CTII (**B**) in 10 mM Tris-HCl, pH 7.5, 0.5 mM EDTA, 1% Triton X-100. In the initial preparation, concentrations of PC and CL were 8.4×10^{-6} M and 4.8×10^{-6} M, respectively. Spectra were recorded at 15 °C for 30 min after adding the indicated increasing amounts of moles of exogenous CL per mol of protein. The spectra at a very top in A and B contained 1% SDS and 9 mol of exogenous CL per mol of protein. Native PAGE (**C**), done according to Segal et al. (1993), included standard proteins from Sigma Chemical Co., St. Louis, MO (A), DCCD-BPF (B), CTII (C), DCCD-BFP with CL (D) and CTII with CL (E). Note: for visual clarity, the lanes that are not essential for the message of this study were cropped from the same Native PAGE as indicated by white vertical lines.

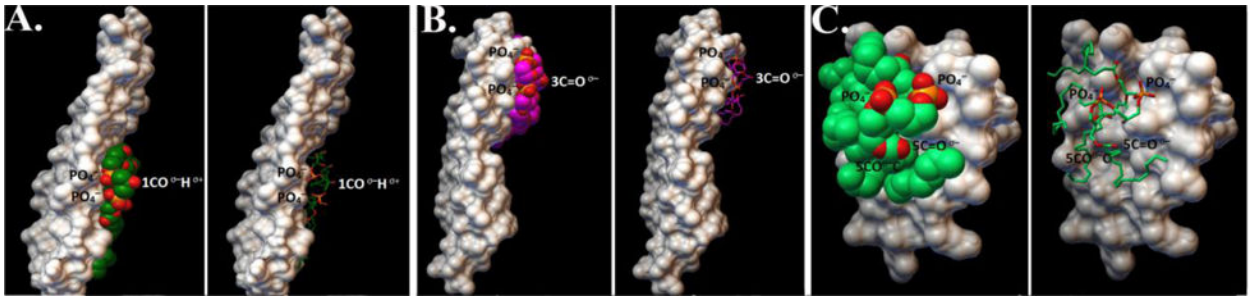

Fig. 6. *In silico* analyses of the interaction of CL to CTII and DCCD-BPF

A) a candidate docked structure showing that the carboxyl group of the polar head of CL are bound to the mid-region of DCCD-BPF in a way that the carboxyl group of CL is facing the aqueous side with an affinity of −3.9 kcal/mol. **B**) Another candidate docked structure showing that the carboxyl group of the polar head of CL are bound at the edge of DCCD-BPF in a way that polar groups of the phospholipid head of CL are facing the aqueous side with a binding affinity of −4.0 kcal/mol. The molecular surface of DCCD-BPF is coloured white whereas the alkyl chains and head groups of CL are shown as sphere or stick model representations. **C**) A candidate docked structure showing that the carboxyl group of the polar head of CL are bound to the three-fingered domain of CTII in a way that polar groups of the phospholipid head of CL are facing the aqueous side with an affinity of −3.5 kcal/mol. For all docked structures molecular surface of DCCD-BPF or CTII is coloured white whereas the alkyl chains and head groups of CL are shown as sphere or stick model representations.

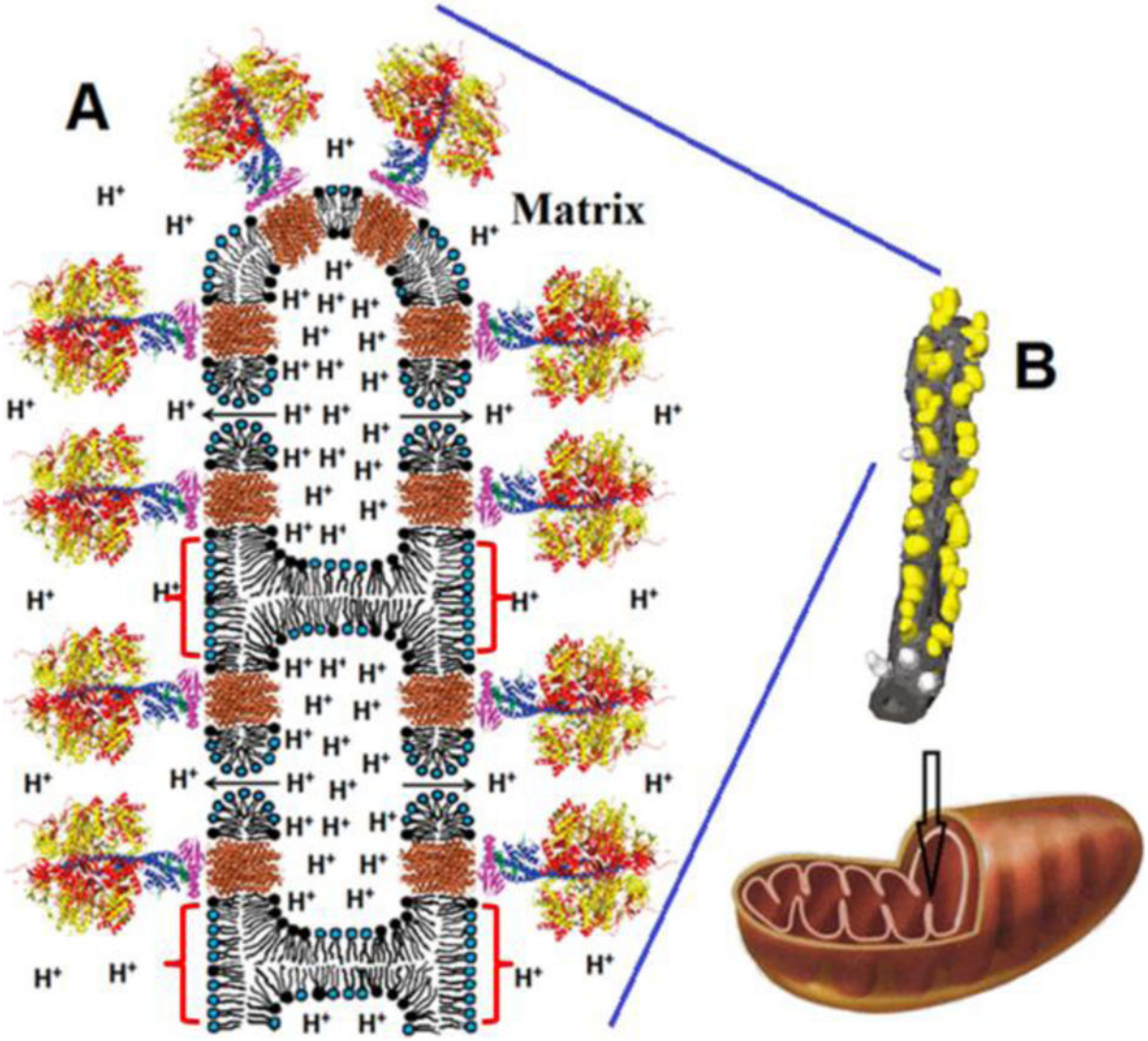

Fig. 7. Schematic representation of an inverted micelle formed between adjacent IMM of a cristae

For simplicity, the inverted micelle includes only four ATP synthases and two toroidal like pores. We suggest that the formation of inverted micelles (shown by red brackets) and toroidal pores may be caused by the low pH when the H^+ concentration is increased in IM space (see text for details). The release of protons from an inverted micelle to matrix occurs via F_0 (shown in brown) and toroidal pores (shown by arrows). Toroidal pores are short-lived transient structures serving to release dangerously high H^+ concentrations. The overall organization of ATP synthases (**A**) is based on the structure modified from Watt et al. 2010 [3]. The α- and β-subunits of catalytic domain are shown in red and yellow respectively. The subunits γ, δ, and ε of the central stalk are depicted in blue, purple, and green. The central stalk and the C-ring (given in brown) together constitute the rotor. Phospholipids with the polar heads (black) represent CL. Phospholipids with blue polar heads represent the other acidic and neutral phospholipids. The image of tubular cristae of mitochondrion (**B**) showing F_1 head dimers on its surface was modified from Strauss et al. 2008 [4]. The F_1 heads are

yellow and the membrane is grey. The F_1 heads not assigned to dimers are shown in lighter grey.